European Journal of Mechanics A/Solids 64 (2017) 29–45

Contents lists available at ScienceDirect

European Journal of Mechanics A/Solids

journal homepage: www.elsevier.com/locate/ejmsol

Vibrating nonlocal multi-nanoplate system under inplane magnetic field

Danilo Karličić [a], Milan Cajić [a], Sondipon Adhikari [b], Predrag Kozić [c], Tony Murmu [d, *]

[a] Mathematical Institute of the Serbian Academy of Sciences and Arts, Kneza Mihaila 36, 11001, Belgrade, Serbia
[b] College of Engineering, Swansea University, Singleton Park, Swansea, SA2 8PP, UK
[c] Faculty of Mechanical Engineering, University of Niš, A. Medvedeva 14, 18000, Niš, Serbia
[d] School of Engineering, University of the West of Scotland, Paisley, PA12BE, UK

ARTICLE INFO

Article history:
Received 10 August 2015
Received in revised form
10 January 2017
Accepted 26 January 2017
Available online 30 January 2017

Keywords:
Nonlocal viscoelasticity
Orthotropic nanoplates
Magnetic field
Multi-layered graphene sheets

ABSTRACT

The recent development in nanotechnology resulted in growing of various nanoplate like structures. High attention was devoted to graphene sheet nanostructure, which enforced the scientist to start developing various theoretical models to investigate its physical properties. Magnetic field effects on nanoplates, especially graphene sheets, have also attracted a considerable attention of the scientific community. Here, by using the nonlocal theory, we examine the influence of in-plane magnetic field on the viscoelastic orthotropic multi-nanoplate system (VOMNPS) embedded in a viscoelastic medium. We derive the system of *m* partial differential equations describing the free transverse vibration of VOMNPS under the uniaxial in-plane magnetic field using the Eringen's nonlocal elasticity and Kirchhoff's plate theory considering the viscoelastic and orthotropic material properties of nanoplates. Closed form solutions for complex natural frequencies are derived by applying the Navier's and trigonometric method for the case of simply supported nanoplates. The results obtained with analytical method are validated with the results obtained by using the numerical method. In addition, numerical examples are given to show the effects of nonlocal parameter, internal damping, damping and stiffness of viscoelastic medium, rotary inertia and uniaxial in-plane magnetic force on the real and the imaginary parts of complex natural frequencies of VOMNPS. This study can be useful as a starting point for the research and design of nanoelectromechanical devices based on graphene sheets.

1. Introduction

Complex nanoscale systems are made of nanostructures with superior thermal, electric, mechanical, magnetic and other physical properties (Hao et al., 2011; Qian et al., 2000; Loomis and Panchapakesan, 2012; Grimes et al., 2000; Sandler et al., 1999) that makes them convenient for potential application in nano-electromechanical systems (NEMS) and micro-electromechanical systems (MEMS) (Loomis et al., 2012a, 2013; Lu and Panchapakesan, 2007a; Lu and Panchapakesan, 2007b; Bunch et al., 2007; Liu et al., 2011). Nanoplate-like nanostructures can be synthetized from different materials to make gold nanoplates, silver nanoplates, boron-nitride sheets, ZnO nanoplates, graphene sheets (Loomis et al., 2012b; Liu et al., 2012; Golberg et al., 2010; Zhang and Huang, 2006; Arani et al., 2014; Meyer et al., 2007; Ramanathan et al., 2008). Studying the vibration behavior of such nanoscale structures may be important step for their optimal application in nanoengineering.

Under complex nanostructure systems we usually mean on nanoscale systems composed of multiple nanorods, nanobeams or nanoplates embedded in certain type of medium. Special class of these systems is multi-nanoplate like system such as multi-layered graphene sheets bonded with certain type of medium. Different studies and research methodologies applied to such systems are presented in the literature by different authors (Stankovich et al., 2006; Shahil and Balandin, 2012; Li et al., 2010; Ansari et al., 2011; Pumera et al., 2010; Lin, 2015; Lin, 2012). In theoretical continuum models of graphene sheets, they are observed as both, isotropic and orthotropic materials. Behfar et al (Behfar and Naghdabadi, 2005). analyzed the vibration behavior of multi-layered graphene sheets system as an orthotropic multi-nanoplate system embedded in elastic medium, where natural

* Corresponding author.
E-mail address: murmutony@gmail.com (T. Murmu).

http://dx.doi.org/10.1016/j.euromechsol.2017.01.013
0997-7538/

frequencies and corresponding modes are found. Arghavan (2012) performed an extensive study on mechanical properties and vibration behavior of graphene sheets also using an orthotropic continuum plate theory to model observed nanostructures. Further, Pradhan et al (Pradhan and Kumar, 2011). employed numerical differential quadrature method to study the vibration of single layered graphene sheets using the nonlocal orthotropic plate theory. Finally, Bu et al (Ni et al., 2010). observed graphene sheets as anisotropic structures and concluded that such properties are attributed to the hexagonal structure of graphene unit cells. They performed molecular dynamics simulations and demonstrated different fractures in longitudinal and transverse modes. However, under certain assumptions and for specific applications, graphene sheets can be observed as isotropic nanoplate structures (Pradhan and Phadikar, 2009; Liang and Han, 2014; Singh and Patel, 2016; Ansari et al., 2010; Murmu and Adhikari, 2011). In this paper, we adopted an orthotropic nonlocal plate theory to model graphene sheets.

When magnetic field is exerted on a conducting nanoplate structure, it can exhibit various dynamical behaviors depending of the magnitude of the field, magnetic permeability of the continuum and deformation regime. Vibration response of carbon nanotubes (CNTs) in the presence of magnetic field is widely examined by many investigators. Murmu et al. (2012a). examined the vibration behavior of a double-walled carbon nanotube subjected to an externally applied longitudinal magnetic field. Based on the nonlocal elasticity theory, Euler–Bernoulli beam model and Maxwell's classical relations, the authors derived a set of two governing equations for transverse vibration of a double walled CNT system. By using the method of separation of variables, they obtained analytical solution for transverse displacements, natural frequencies and amplitude ratios. They have shown that the applied longitudinal magnetic field has a strong influence on the dynamic behavior of a double-walled CNT system. In (Murmu et al., 2012b), the same authors presented a mechanical model of two single-walled CNTs coupled with elastic medium and influenced by the longitudinal magnetic field. They derived governing equations for the free vibrations and analytically obtained nonlocal natural frequencies of the system using the Eringen's nonlocal elasticity theory, Euler–Bernoulli beam model and Maxwell's relations. Kiani (2014a) analyzed the vibration and instability behavior of a single-walled CNT under a general magnetic field. By using the nonlocal Rayleigh beam theory and Maxwell's relations, the dimensionless governing equation for the free vibration of the system is derived considering a general magnetic field. The longitudinal and flexural frequencies are obtained analytically and effects of the longitudinal and transverse magnetic fields are shown through several numerical examples. Further, Narendar et al. (2012). studied the wave propagation in a single-walled CNT under longitudinal magnetic field. The authors derived nonlocal governing differential equation considering the Maxwell's equations, nonlocal elasticity theory and Euler–Bernoulli beam model. The wave propagation analysis is performed using the spectral analysis. It is found that nonlocal effects reduces the wave velocity irrespective of the presence of a magnetic field and doesn't have an influence on it in the higher frequency region. Recently, several theoretical studies of nanoplates under the influence of magnetic field are performed. Murmu et al. (2013). studied the transverse vibration of a single-layer graphene sheet (SLGS) embedded in elastic medium and under the influence of in-plane magnetic field by using the nonlocal theory. The authors have examined the effects of nonlocal parameter and in-plane magnetic field on natural frequencies for different aspect ratios of SLGS. Explicit expressions for natural frequencies were derived analytically. Ghorbanpour Arani et al. (2013). investigated the influence of in-plane two-dimensional magnetic field and biaxial preload on vibration of a double orthotropic graphene sheet system coupled with Pasternak type of elastic layer. The thermo-nonlocal elasticity theory and Maxwell's relations are used to derive governing equations of the system. In addition, the differential quadrature method (DQM) is employed in order to solve the equations. The effects of magnetic field, in-plane preload, nonlocal parameter and different aspect ratios on frequencies of graphene sheets were examined. The free in-plane and out-of-plane vibration study of a rectangular nanoplate under the influence of unidirectional in-plane magnetic field was conducted by Kiani (2014b). The authors employed Kirchhoff, Mindlin and higher order plate theories using the nonlocal elasticity theory. The effects of small-scale parameter, magnetic field and aspect ratios on natural frequencies of the in-plane and out-of-plane vibrations were investigated. The reason for different properties and dynamic behavior of nanostructures in the presence of magnetic field is due to acting electromagnetic forces on each element of a structure. It should be noted that by considering the Maxwell's equations and Lorentz's forces, one could form relations between forces acting on each particle of a nanostructure and vector magnetic field.

Until now, there is no experimental work reported in the literature regarding to the vibration behavior of multi-nano-beam/plates system under the influence of magnetic field. Nevertheless, some experiments have shown that certain physical and mechanical properties are changing and some specific phenomena's appears in CNTs and graphene sheets when a magnetic field is applied on them (Camponeschi et al., 2007; Kiani, 2014c; Fujiwara et al., 2001; Peng, 2011; Shizuya, 2007; Fu et al., 2011; Lopez-Urias et al., 2006; Faugeras et al., 2010; Kan et al., 2008; Nair et al., 2013; Ning et al., 2013; Olsen et al., 2013; Pesin and MacDonald, 2012; Yazyev, 2010; Wang et al., 2009). In addition, there are some reports (Garmestani et al., 2003; Ahir et al., 2008; Kimura et al., 2002) about the alignment of carbon nanotubes (CNTs) when magnetic field is exerted on arbitrary placed ensembles of CNTs. In general, it is not an easy task to perform experiments on nanoscale level owing to the weak control of parameters. Atomistic simulation methods can be very efficient for the investigation of the mechanical behavior of nanostructures. However, such methods are computationally prohibitive for complex nanoscale systems since a large number of atoms need to be considered in the simulations. Finally, continuum based methods seems to be a logical tool utilized in the theoretical investigation of the mechanical behavior of complex nanostructure systems. Nevertheless, classical continuum theory neglects the interatomic interactions and thus, it needs to be modified to consider such effects. Such modifications were conducted by Kröner (1967) and Eringen (1972) using the integral forms in the stress-strain relation. Here, we will utilize the Eringen nonlocal differential form of equation (Eringen, 1983), which accounts for the small-size effects trough a single parameter. In the literature, there are numerous of studies on vibration behavior of nanostructures using the nonlocal theory (Peddieson et al., 2003; Wang and Liew, 2007; Murmu and Adhikari, 2010; Reddy, 2007; Huu-Tai, 2012; Wang et al., 2011; Arash and Wang, 2014; Malekzadeh and Shojaee, 2013; Mohammadi et al., 2013).

By browsing the literature, it is found that the free vibration problem of a multiple-nanostructure system is analytically treated in a small number of papers. The presented dynamical model of a multiple graphene sheets system can be important step in design of complex NEMS devices and nanocomposites, so this paper aims to fill the gap by providing the analytical results for futures studies in nanoengineering practice. In the following, we utilize the nonlocal theory to investigate the free vibration behavior of VOMNPS embedded in a viscoelastic medium and subjected to the in-plane magnetic field. For the mechanical model of a graphene sheet, we

used a nonlocal Kirchhoff's plate theory. Lorentz forces induced in nanoplates by an applied magnetic field are determined through Maxwell's equations. In this study, we adopted the simply supported boundary conditions for nanoplates. By using the trigonometric method, we obtain closed form expressions for complex natural frequencies of the free transversally vibrating VOMNPS coupled in three different "chain" conditions, "Clamped-Chain", "Cantilever-Chain" and "Free-Chain". In addition, an asymptotic analysis is performed in order to determine critical complex natural frequencies of the system. Analytical results are validated with the results obtained by using the numerical method. Further, a detailed parametric study is conducted for VOMNPS representing the system of multiple graphene sheets embedded in a polymer matrix. The effects of change of nonlocal parameter, magnitude of magnetic field and a number of nanoplates on complex natural frequencies of VOMNPS are investigated for variety of parameters.

2. Maxwell's relation

According to the classical Maxwell relation (Arani et al., 2013), the relationships between the current density **J**, distributing vector of magnetic field **h**, strength vectors of the electric fields **e** and magnetic field permeability η are represented by Maxwell's equations in differential form and can be retrieved as

$$\mathbf{J} = \nabla \times \mathbf{h}, \quad \nabla \times \mathbf{e} = -\eta \frac{\partial \mathbf{h}}{\partial t}, \quad \nabla \cdot \mathbf{h} = 0, \tag{1}$$

where vectors of distributing magnetic field **h** and the electric field **e** are defined as

$$\mathbf{h} = \nabla \times (\mathbf{U} \times \mathbf{H}), \quad \mathbf{e} = -\eta \left(\frac{\partial \mathbf{U}}{\partial t} \times \mathbf{H} \right). \tag{2}$$

In the above equation, $\nabla = \frac{\partial}{\partial x}\mathbf{i} + \frac{\partial}{\partial y}\mathbf{j} + \frac{\partial}{\partial z}\mathbf{k}$ is the Hamilton operator, $\mathbf{U}(x,y,z) = \overline{u}_{ix}\mathbf{i} + \overline{v}_{iy}\mathbf{j} + \overline{w}_{iz}\mathrm{k}$ is the displacement vector and $\mathbf{H} = (H_x, 0, 0)$ is the vector of the in-plane magnetic field. It is assumed that the in-plane magnetic field acts on VOMNPS in the x-direction of each nanoplate. We can write the vector of the distributing magnetic field in the following form

$$\mathbf{h} = -H_x \left(\frac{\partial \overline{v}_{iy}}{\partial y} + \frac{\partial \overline{w}_{iz}}{\partial z} \right) \mathbf{i} + H_x \frac{\partial \overline{v}_{iy}}{\partial x} \mathbf{j} + H_x \frac{\partial \overline{w}_{iz}}{\partial x} \mathbf{k}. \tag{3}$$

Introducing Eq. (3) into the first expressions of Eq. (1) one obtains

$$\begin{aligned} \mathbf{J} = \nabla \times \mathbf{h} = H_x \left(-\frac{\partial^2 \overline{v}_{iy}}{\partial x \partial z} + \frac{\partial^2 \overline{w}_{iz}}{\partial x \partial y} \right) \mathbf{i} - H_x \left(\frac{\partial^2 \overline{v}_{iy}}{\partial y \partial z} + \frac{\partial^2 \overline{w}_{iz}}{\partial x^2} + \frac{\partial^2 \overline{w}_{iz}}{\partial z^2} \right) \mathbf{j} \\ + H_x \left(\frac{\partial^2 \overline{v}_{iy}}{\partial x^2} + \frac{\partial^2 \overline{v}_{iy}}{\partial y^2} + \frac{\partial^2 \overline{w}_{iz}}{\partial z \partial y} \right) \mathbf{k}. \end{aligned} \tag{4}$$

Further, using Eq. (4) into the expressions for the Lorentz forces induced by the in-plane uniaxial magnetic field, yields

$$\begin{aligned} \mathbf{f}\left(f_x, f_y, f_z\right) = \eta(\mathbf{J} \times \mathbf{H}) = \eta \Bigg[0\mathbf{i} + H_x^2 \left(\frac{\partial^2 \overline{v}_{iy}}{\partial x^2} + \frac{\partial^2 \overline{v}_{iy}}{\partial y^2} + \frac{\partial^2 \overline{w}_{iz}}{\partial z \partial y} \right) \mathbf{j} \\ + H_x^2 \left(\frac{\partial^2 \overline{w}_{iz}}{\partial x^2} + \frac{\partial^2 \overline{w}_{iz}}{\partial z^2} + \frac{\partial^2 \overline{v}_{iy}}{\partial z \partial y} \right) \mathbf{k} \Bigg]. \end{aligned} \tag{5}$$

Here f_x, f_y and f_z are the Lorentz forces along the x, y and z directions, respectively of the form

$$f_{x,i} = 0, \tag{6a}$$

$$f_{y,i} = \eta H_x^2 \left(\frac{\partial^2 \overline{v}_{iy}}{\partial x^2} + \frac{\partial^2 \overline{v}_{iy}}{\partial y^2} + \frac{\partial^2 \overline{w}_{iz}}{\partial z \partial y} \right), \tag{6b}$$

$$f_{z,i} = \eta H_x^2 \left(\frac{\partial^2 \overline{w}_{iz}}{\partial x^2} + \frac{\partial^2 \overline{w}_{iz}}{\partial z^2} + \frac{\partial^2 \overline{v}_{iy}}{\partial z \partial y} \right). \tag{6c}$$

In this study, we assume Kirchhoff displacement field $\left(\overline{u}_{ix} = -z\frac{\partial w_i(x,y,t)}{\partial x}, \quad \overline{v}_{iy} = -z\frac{\partial w_i(x,y,t)}{\partial y}, \quad \overline{w}_{iz} = w_i(x,y,t) \right)$ and the Lorentz forces as

$$f_{x,i} = 0, \tag{7a}$$

$$f_{y,i} = -z\eta H_x^2 \left(\frac{\partial^3 w_i}{\partial y^3} + \frac{\partial^3 w_i}{\partial x^2 \partial y} \right), \tag{7b}$$

$$f_{z,i} = \eta H_x^2 \left(\frac{\partial^2 w_i}{\partial x^2} - \frac{\partial^2 w_i}{\partial y^2} \right). \tag{7c}$$

Now, it is possible to obtain generated in-plane force $\mathbf{F_m} = \int_{-h/2}^{h/2} \mathbf{f}\, dz$ and bending moment $\mathbf{M_m} = \int_{-h/2}^{h/2} z\, \mathbf{f} dz$, which acts on the i-th nanoplate as

$$\mathbf{F_m} = \int_{-h/2}^{h/2} \mathbf{f}\, dz = 0\mathbf{i} + 0\mathbf{j} + \eta h H_x^2 \left(\frac{\partial^2 w_i}{\partial x^2} - \frac{\partial^2 w_i}{\partial y^2} \right) \mathbf{k}, \tag{8a}$$

$$\mathbf{M_m} = \int_{-h/2}^{h/2} z\, \mathbf{f} dz = 0\mathbf{i} - \frac{\eta h^3 H_x^2}{12} \left(\frac{\partial^3 w_i}{\partial y^3} + \frac{\partial^3 w_i}{\partial x^2 \partial y} \right) \mathbf{j} + 0\mathbf{k}. \tag{8b}$$

It should be note that influences of the bending moments Eq. (8) can be neglected since in the following we consider only thin plate theory for nanoplates, as shown in (Kiani, 2014c).

3. Nonlocal viscoelastic constitutive relation

In this section, we will consider the basic equation of nonlocal elasticity and viscoelasticity in the general and two-dimensional case. In (Eringen, 1972), a constitutive relation for nonlocal stress tensor at a point $\boldsymbol{x}$ is derived in its integral formulation based on the assumption that the stress at a point is a function of the strains at all points of an elastic body. Fundamental form of the nonlocal elastic constitutive relation for a three-dimensional linear, homogeneous isotropic body is expressed as

$$\sigma_{ij}(\boldsymbol{x}) = \int \alpha(|\boldsymbol{x} - \boldsymbol{x}'|, \tau) C_{ijkl} \varepsilon_{kl}(\boldsymbol{x}') dV(\boldsymbol{x}'), \forall \boldsymbol{x} \in V, \tag{9a}$$

$$\sigma_{ij,j} = 0, \tag{9b}$$

$$\varepsilon_{ij} = \frac{1}{2}(u_{i,j} + u_{j,i}), \tag{9c}$$

where C_{ijkl} is the elastic modulus tensor for classical isotropic elasticity; σ_{ij} and ε_{ij} are the stress and the strain tensors, respectively, and u_i is the displacement vector. With $\alpha(|x - x'|, \tau)$ we denote the nonlocal modulus or attenuation function, which incorporates nonlocal effects into the constitutive equation at a reference point x produced by the local strain at a source x'. The

above absolute value of the difference $|x - x'|$ denotes the Euclidean metric. The parameter τ is equal to $\tau = (e_0\tilde{a})/l$ where l is the external characteristic length (crack length, wave length), $\tilde{a}$ describes the internal characteristic length (lattice parameter, granular size and distance between C–C bounds) and e_0 is a constant appropriate to each material that can be identified from atomistic simulations or by using the dispersive curve of the Born-Karman model of lattice dynamics.

Because of difficulties arising in the analytical analysis of continuum systems with integral form of constitutive equation, in (Eringen, 1983) this form has been reformulated into the differential form of constitutive equation by adopting specific kernel functions. Differential form is proved to be very efficient, simple, and convenient for analytical techniques of solving different vibration and stability analysis problems in nanostructure based systems. The differential form of the nonlocal constitutive relation is given as

$$\left(1 - \mu\nabla^2\right)\sigma_{ij} = t_{ij}, \tag{10}$$

where $\nabla^2 = \cdot = \frac{d^2}{dx^2} + \frac{d^2}{dy^2}$ is the Laplacian;$\mu = (e_0\tilde{a})^2$ is the nonlocal parameter; and $t_{ij} = C_{ijkl}\varepsilon_{kl}$ is the classical stress tensor. From Eq. (10), the constitutive relations for homogeneous elastic nanoplates can be expressed as

$$\left(1 - \mu\ \nabla^2\right)\begin{pmatrix}\sigma_{xx}\\ \sigma_{yy}\\ \tau_{xy}\end{pmatrix} = \begin{bmatrix}\frac{E}{1-\vartheta^2} & \frac{\vartheta E}{1-\vartheta^2} & 0\\ \frac{\vartheta E}{1-\vartheta^2} & \frac{E}{1-\vartheta^2} & 0\\ 0 & 0 & G\end{bmatrix}\begin{pmatrix}\varepsilon_{xx}\\ \varepsilon_{yy}\\ \gamma_{xy}\end{pmatrix}, \tag{11}$$

where E, G and ϑ are the Young's modulus, shear modulus and Poisson's ratio, respectively.

The nonlocal viscoelastic constitutive relation for Kelvin-Voigt viscoelastic nanoplate proposed in paper (Pouresmaeeli et al., 2013) is a combination of nonlocal elasticity and viscoelasticity theory. For the case of two - dimensional nonlocal viscoelastic orthotropic nanoplates constitutive relations are given as

$$(1 - \mu\ \Delta)\begin{pmatrix}\sigma_{xx}\\ \sigma_{yy}\\ \tau_{xy}\end{pmatrix} = \begin{bmatrix}\frac{E_1\left(1+\tau_d\frac{\partial}{\partial t}\right)}{1-\vartheta_{12}\vartheta_{21}} & \frac{\vartheta_{12}E_1\left(1+\tau_d\frac{\partial}{\partial t}\right)}{1-\vartheta_{12}\vartheta_{21}} & 0\\ \frac{\vartheta_{12}E_2\left(1+\tau_d\frac{\partial}{\partial t}\right)}{1-\vartheta_{12}\vartheta_{21}} & \frac{E_2\left(1+\tau_d\frac{\partial}{\partial t}\right)}{1-\vartheta_{12}\vartheta_{21}} & 0\\ 0 & 0 & G_{12}\left(1+\tau_d\frac{\partial}{\partial t}\right)\end{bmatrix}\begin{pmatrix}\varepsilon_{xx}\\ \varepsilon_{yy}\\ \gamma_{xy}\end{pmatrix}, \tag{12}$$

where τ_d is the internal damping coefficient of nanobeam, E_1 , E_2 and ϑ_{12}, ϑ_{21} are Young's modulus's and Poisson's ratios, respectively in two orthogonal directions. If $\tau_d = 0$ i.e. by neglecting the internal viscosity, we than obtain the constitutive relation for nonlocal elasticity. In the follow, we use the constitutive relation for nonlocal viscoelasticity in Eq. (12) to derive governing equations of motion.

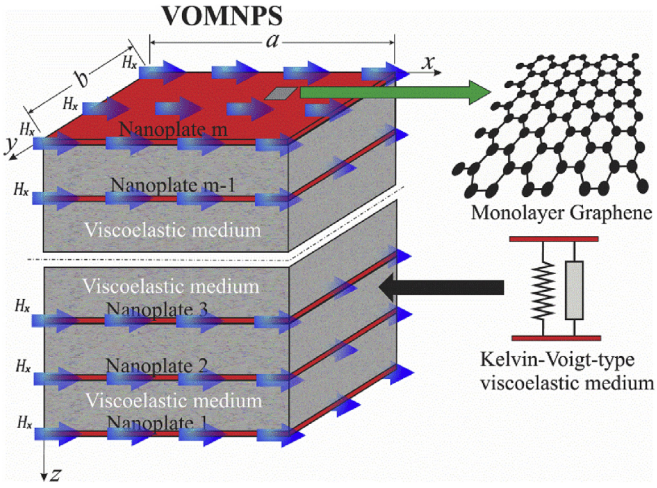

Fig. 1. VOMNPS embedded in a viscoelastic medium and under the influence of uniaxial in-plane magnetic field H_x.

4. Structural problem formulation

Here, we consider the free vibration of VOMNPS composed of m orthotropic viscoelastic nanoplates embedded in Kelvin-Voigt-type viscoelastic medium and under the in-plane uniaxial magnetic field, as shown in Fig. 1. The VOMNPS is modeled as a stack of rectangular simply supported orthotropic nanoplates with same material and geometrical characteristics, with elastic modulus E_1 and E_2, Poison coefficients ϑ_{12} and ϑ_{21}, shear modulus G_{12}, internal damping parameter τ_d, mass density ρ, length a, width b and thickness h. Viscoelastic medium located between nanoplates of VOMNPS is modeled via continuously distributed pairs of parallelly connected springs and dampers, also known as Kelvin-Voigt model of viscoelasticity, with stiffness coefficients k_i and damping coefficients b_i. It should be noted that each nanoplate in VOMNPS is subjected to the in-plane uniaxial magnetic field in the x direction. We assume that transversal displacements of nanoplates are $w_1(x,y,t)$, $w_2(x,y,t)$, $w_3(x,y,t)$, $w_4(x,y,t)$ … $w_m(x,y,t)$.

Using the classical plate theory, displacement components in x, y and z direction for an arbitrary point of the i-th nanoplate can be expressed as (Reddy, 2006):

$$\overline{u}_{ix} = u_i(x,y,t) - z\frac{\partial w_i(x,y,t)}{\partial x}, \quad \overline{v}_{iy} = v_i - z\frac{\partial w_i(x,y,t)}{\partial y}, \quad \overline{w}_{iz} = w_i(x,y,t), \tag{13}$$

where u_i, v_i and w_i are the displacements of nanoplates in the x, y and z directions, respectively. By using Eq. (13), the strain - displacement relations of the linear strain theory (Reddy, 2006) are

$$\varepsilon_{xx} = \frac{\partial u_i}{\partial x} - z\frac{\partial^2 w_i}{\partial x^2}, \quad \varepsilon_{yy} = \frac{\partial v_i}{\partial x} - z\frac{\partial^2 w_i}{\partial y^2}, \quad \gamma_{xy} = \frac{\partial u_i}{\partial y} + \frac{\partial v_i}{\partial x} - 2z\frac{\partial^2 w_i}{\partial x \partial y}, \tag{14a}$$

$$\varepsilon_{zz} = \frac{\partial w_i}{\partial z} = 0, \quad \gamma_{xz} = \frac{\partial \overline{u}_{ix}}{\partial z} + \frac{\partial \overline{w}_{iz}}{\partial x} = 0, \quad \gamma_{yz} = \frac{\partial \overline{v}_{ix}}{\partial z} + \frac{\partial \overline{w}_{iz}}{\partial y} = 0, \tag{14b}$$

where ε_{xx}, ε_{yy} and ε_{zz} are the normal strains, and γ_{xy}, γ_{xz} and γ_{yz} are the shear strains. Based on the Newton's second law for the infinitesimal element of the *i-th* nanoplate, equilibrium equations can be obtained in the following form

$$q + \frac{\partial Q_x}{\partial x} + \frac{\partial Q_y}{\partial y} = \rho h \frac{\partial^2 w_i}{\partial t^2}, \tag{15a}$$

$$\frac{\partial M_{xx}}{\partial x} + \frac{\partial M_{xy}}{\partial y} + \frac{\rho h^3}{12}\frac{\partial^3 w_i}{\partial t^2 \partial x} = Q_x, \tag{15b}$$

$$\frac{\partial M_{yy}}{\partial y} + \frac{\partial M_{xy}}{\partial x} + \frac{\rho h^3}{12}\frac{\partial^3 w_i}{\partial t^2 \partial y} = Q_y, \tag{15c}$$

$$\frac{\partial N_{xx}}{\partial x} + \frac{\partial N_{xy}}{\partial y} = \rho h \frac{\partial^2 u_i}{\partial t^2}, \tag{15d}$$

$$\frac{\partial N_{yy}}{\partial y} + \frac{\partial N_{xy}}{\partial x} = \rho h \frac{\partial^2 v_i}{\partial t^2}, \tag{15e}$$

in which $\partial w_i/\partial x$ and $\partial w_i/\partial y$ are angles of rotation, $\rho h^3/12$ is the rotary inertia, N_{xx}, N_{yy} and N_{xy} are the in-plane stress resultants M_x, M_y and M_{xy} are the moment resultants, and Q_x and Q_y are the transverse shearing resultants, which are defined as

$$(N_{xx}, N_{yy}, N_{xy} M_x, M_y, M_{xy}, Q_x, Q_y) = \int_{-h/2}^{h/2} (\sigma_{xx}, \sigma_{yy}, \tau_{xy}, z\sigma_{xx}, z\sigma_{yy}, z\tau_{xy}, \ \tau_{xz}, \tau_{yz}) dz. \tag{16}$$

Introducing Eqs. (15b) and (15c) into Eq. (15a), and neglecting the in-plane displacements u_i and v_i, we obtain the following motion equation of the *i-th* nanoplate in terms of the stress couple resultants

$$q + \frac{\partial^2 M_{xx}}{\partial x^2} + \frac{\partial^2 M_{yy}}{\partial y^2} + 2\frac{\partial^2 M_{xy}}{\partial x \partial y} = \rho h \frac{\partial^2 w_i}{\partial t^2} - \frac{\rho h^3}{12}\left(\frac{\partial^4 w_i}{\partial t^2 \partial x^2} + \frac{\partial^4 w_i}{\partial t^2 \partial y^2}\right), \tag{17}$$

in which $q(x, y, t)$ is external force caused by viscoelastic medium and in-plane uniaxial magnetic force (Fig. 1b) of the form

$$q(x, y, t) = F_{ki} - F_{ki-1} + \eta h H_x^2 \left(\frac{\partial^2 w_i}{\partial x^2} - \frac{\partial^2 w_i}{\partial y^2}\right), \tag{18}$$

where

$$F_{ki} = k_i(w_{i+1} - w_i) + b_i(\dot{w}_{i+1} - \dot{w}_i), \quad F_{ki-1} = k_{i-1}(w_i - w_{i-1}) + b_{i-1}(\dot{w}_i - \dot{w}_{i-1}). \tag{19}$$

Introducing Eq. (14a) into Eq. (12) and using expression (16), yields

$$(1 - \mu\ \Delta)M_{xx} = -D_{11}\left(1 + \tau_d\frac{\partial}{\partial t}\right)\frac{\partial^2 w_i}{\partial x^2} - D_{12}\left(1 + \tau_d\frac{\partial}{\partial t}\right)\frac{\partial^2 w_i}{\partial y^2}, \tag{20a}$$

$$(1 - \mu\ \Delta)M_{yy} = -D_{12}\left(1 + \tau_d\frac{\partial}{\partial t}\right)\frac{\partial^2 w_i}{\partial x^2} - D_{22}\left(1 + \tau_d\frac{\partial}{\partial t}\right)\frac{\partial^2 w_i}{\partial y^2}, \tag{20b}$$

$$(1 - \mu\ \Delta)M_{xy} = -2D_{66}\left(1 + \tau_d\frac{\partial}{\partial t}\right)\frac{\partial^2 w_i}{\partial x \partial y}, \tag{20c}$$

where D_{11}, D_{12}, D_{22} and D_{66} are the bending rigidities of orthotropic viscoelastic nanoplates which are expressed as

$$D_{11} = \frac{E_1 h^3}{12(1 - \vartheta_{12}\vartheta_{21})}, \quad D_{12} = \frac{\vartheta_{12} E_2 h^3}{12(1 - \vartheta_{12}\vartheta_{21})}, \quad D_{22} = \frac{E_2 h^3}{12(1 - \vartheta_{12}\vartheta_{21})}, \quad D_{66} = \frac{G_{12} h^3}{12}. \tag{21}$$

Finally, by using Eqs. (17) and (20), we obtain governing equations of motion in terms of transversal displacement of the *i-th* nanoplate in the following form

$$\begin{aligned}
&\rho h \frac{\partial^2 w_i}{\partial t^2} - \frac{\rho h^3}{12}\left(\frac{\partial^4 w_i}{\partial t^2 \partial x^2} + \frac{\partial^4 w_i}{\partial t^2 \partial y^2}\right) - \eta h H_x^2 \left(\frac{\partial^2 w_i}{\partial x^2} - \frac{\partial^2 w_i}{\partial y^2}\right) \\
&\quad + k_i(w_i - w_{i+1}) + b_i\left(\frac{\partial w_i}{\partial t} - \frac{\partial w_{i+1}}{\partial t}\right) + k_{i-1}(w_i - w_{i-1}) \\
&\quad + b_{i-1}\left(\frac{\partial w_i}{\partial t} - \frac{\partial w_{i-1}}{\partial t}\right) + D_{11}\left(1 + \tau_d\frac{\partial}{\partial t}\right)\frac{\partial^4 w_i}{\partial x^4} \\
&\quad + D_{22}\left(1 + \tau_d\frac{\partial}{\partial t}\right)\frac{\partial^4 w_i}{\partial y^4} + 2(D_{12} + 2D_{66})\left(1 + \tau_d\frac{\partial}{\partial t}\right) \\
&\quad \frac{\partial^2 w_i}{\partial x^2 \partial y^2} = \mu\left(\frac{\partial^2}{\partial x^2} + \frac{\partial^2}{\partial y^2}\right)\Bigg[\rho h \frac{\partial^2 w_i}{\partial t^2} - \frac{\rho h^3}{12}\left(\frac{\partial^4 w_i}{\partial t^2 \partial x^2}\right. \\
&\quad \left. + \frac{\partial^4 w_i}{\partial t^2 \partial y^2}\right) - \eta h H_x^2 \left(\frac{\partial^2 w_i}{\partial x^2} - \frac{\partial^2 w_i}{\partial y^2}\right) + k_i(w_i - w_{i+1}) \\
&\quad + b_i\left(\frac{\partial w_i}{\partial t} - \frac{\partial w_{i+1}}{\partial t}\right) + k_{i-1}(w_i - w_{i-1}) \\
&\quad + b_{i-1}\left(\frac{\partial w_i}{\partial t} - \frac{\partial w_{i-1}}{\partial t}\right)\Bigg],
\end{aligned} \tag{22}$$

or in the dimensionless form

$$\frac{\partial^2 \overline{w}_i}{\partial \tau^2} - \frac{\delta^2}{12}\left(\frac{\partial^4 \overline{w}_i}{\partial \tau^2 \partial \xi^2} + R^2 \frac{\partial^4 \overline{w}_i}{\partial \tau^2 \partial \zeta^2}\right) - MP\left(\frac{\partial^2 \overline{w}_i}{\partial \xi^2} - R^2 \frac{\partial^2 \overline{w}_i}{\partial \zeta^2}\right) + K_i(\overline{w}_i - \overline{w}_{i+1}) + B_i\left(\frac{\partial \overline{w}_i}{\partial \tau} - \frac{\partial \overline{w}_{i+1}}{\partial \tau}\right) + K_{i-1}(\overline{w}_i - \overline{w}_{i-1}) + B_{i-1}\left(\frac{\partial \overline{w}_i}{\partial \tau} - \frac{\partial \overline{w}_{i-1}}{\partial \tau}\right) + \left(1 + T_d \frac{\partial}{\partial \tau}\right)\frac{\partial^4 \overline{w}_i}{\partial \xi^4} + Z_{22} R^4 \left(1 + T_d \frac{\partial}{\partial \tau}\right)\frac{\partial^4 \overline{w}_i}{\partial \zeta^4} + 2R^2(Z_{12} + 2Z_{66})\left(1 + T_d \frac{\partial}{\partial \tau}\right)\frac{\partial^2 \overline{w}_i}{\partial \xi^2 \partial \zeta^2} = \eta^2\left(\frac{\partial^2}{\partial \xi^2} + R^2 \frac{\partial^2}{\partial \zeta^2}\right)\left[\frac{\partial^2 \overline{w}_i}{\partial \tau^2} - \frac{\delta^2}{12}\left(\frac{\partial^4 \overline{w}_i}{\partial \tau^2 \partial \xi^2} + R^2 \frac{\partial^4 \overline{w}_i}{\partial \tau^2 \partial \zeta^2}\right) - MP\left(\frac{\partial^2 \overline{w}_i}{\partial \xi^2} - R^2 \frac{\partial^2 \overline{w}_i}{\partial \zeta^2}\right) + K_i(\overline{w}_i - \overline{w}_{i+1}) + B_i\left(\frac{\partial \overline{w}_i}{\partial \tau} - \frac{\partial \overline{w}_{i+1}}{\partial \tau}\right) + K_{i-1}(\overline{w}_i - \overline{w}_{i-1}) + B_{i-1}\left(\frac{\overline{w}_i}{\partial \tau} - \frac{\overline{w}_{i-1}}{\partial \tau}\right)\right], \tag{23}$$

for $i = 1, 2, 3\ldots, m$, where dimensionless parameters are defined as

$$K_i = k_i \frac{a^4}{D_{11}}, \quad B_i = b_i \frac{a^2}{\sqrt{\rho h D_{11}}}, \quad T_d = \tau_d \sqrt{\frac{D_{11}}{a^4 \rho h}}, \quad \eta^2 = \frac{\mu}{a^2}, \quad \tau = t\sqrt{\frac{D_{11}}{a^4 \rho h}}, \quad MP = \frac{\eta h H_x^2 a^2}{D_{11}},$$
$$Z_{22} = \frac{D_{22}}{D_{11}}, \quad Z_{12} = \frac{D_{12}}{D_{11}}, \quad Z_{66} = \frac{D_{66}}{D_{11}}, \quad R = \frac{a}{b}, \quad \delta = \frac{h}{a}, \quad \overline{w}_i = \frac{w_i}{a}, \quad \xi = \frac{x}{a}, \quad \zeta = \frac{y}{b}. \tag{24}$$

Assuming the simply supported boundary conditions for all nanoplates in VOMNPS, we can write the following mathematical expressions

$$w_i(x, 0, t) = w_i(x, b, t) = 0, \quad w_i(0, y, t) = w_i(a, y, t) = 0, \quad i = 1, 2, 3, .., m. \tag{25a}$$

$$M_{xxi}(0, y, t) = M_{xxi}(a, y, t) = 0, \quad M_{yyi}(x, 0, t) = M_{yyi}(x, b, t) = 0. \tag{25b}$$

From a physical point of view, this means that the deflections and moments at all four edges of nanoplates are equal to zero.

5. Exact solutions for complex natural frequencies

In this study we assumed analytical solutions in the form of double Fourier series in which transverse displacement w_i is expanded into a double trigonometric series in terms of unknown parameters as shown in [76, 77]. Considering that the nanoplates in VOMNPS are simply supported Eq. (25), assumed solution for the *i-th* nanoplate is of the form

$$\overline{w}_i(\xi, \zeta, \tau) = \sum_{r=1}^{\infty}\sum_{n=1}^{\infty} W_{irn} \sin(\alpha_r \xi)\sin(\beta_n \zeta) e^{j\Omega_{rn}\tau}, i = 1, 2, 3, .., m, \tag{26}$$

where $j = \sqrt{-1}$, $\alpha_r = r\pi$; $\beta_n = n\pi$ $(r, n = 1, 2, 3, \ldots)$; W_{irn}, Ω_{rn} $(i = 1, 2, 3, .., m)$ are amplitudes and complex natural frequencies, respectively. In the papers (Behfar and Naghdabadi, 2005; Reddy, 2006; Lu et al., 2007) assumed displacement field satisfies the given boundary conditions, and it is independent of the influence of other nanoplates in multi-nanoplate system.

In the continuation of this study, we will consider three cases of coupling of VOMNPS with a fixed base and corresponding exact closed form solutions for complex natural frequencies.

5.1. "Clamped-Chain" system

In the case of "Clamped-Chain" system, the first and the last nanoplate in the model of VOMNPS are connected with the fixed base through the viscoelastic medium represented by layers with stiffness coefficients k_0 and k_m and damping coefficients b_0 and b_m as shown in Fig. 2. Coupling conditions for this chain system in dimensionless form are

$$\overline{w}_0(\xi, \zeta, \tau) = 0, \quad \overline{w}_{m+1}(\xi, \zeta, \tau) = 0. \tag{27}$$

By introducing expression for coupling condition (27) and assumed solution Eq. (26) into the equation of motion Eq. (23) of VOMNPS and assuming that the stiffness and damping coefficients of viscoelastic medium are identical $K_0 = K_1 = \ldots = K_m = K$ and $B_0 = B_1 = \ldots = B_m = B$, we obtain the system of algebraic equations

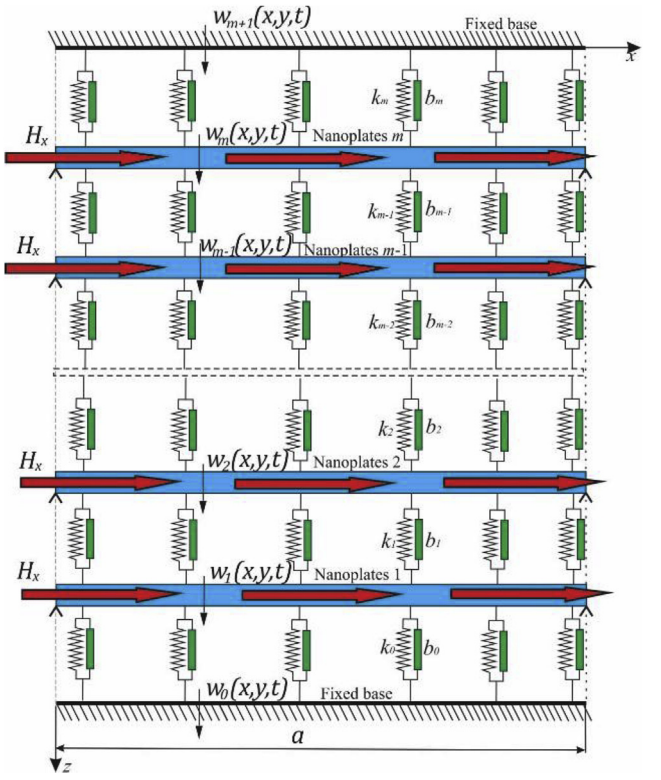

Fig. 2. Side view of VOMNPS embedded in the viscoelastic medium and under the influence of uniaxial in-plane magnetic field, "Clamped-Chain" system.

in the following form

$$\widehat{S}_{rn}W_{1rn} - \widehat{v}_{rn}W_{2rn} = 0, \quad i = 1, \tag{28a}$$

$$-\widehat{v}_{rn}W_{i-1rn} + \widehat{S}_{rn}W_{irn} - \widehat{v}_{rn}W_{i+1rn} = 0, \quad i = 2, 3, .., m-1, \tag{28b}$$

$$-\widehat{v}_{rn}W_{m-1rn} + \widehat{S}_{rn}W_{mrn} = 0, \quad i = m, \tag{28c}$$

or in the matrix form

$$\begin{bmatrix} \widehat{S}_{rn} & -\widehat{v}_{rn} & 0 & \dots & 0 & 0 & 0 & \dots & 0 & 0 & 0 \\ -\widehat{v}_{rn} & \widehat{S}_{rn} & -\widehat{v}_{rn} & \dots & 0 & 0 & 0 & \dots & 0 & 0 & 0 \\ \dots & \dots & \dots & \dots & \dots & \dots & \dots & \dots & \dots & \dots & \dots \\ 0 & 0 & 0 & \dots & \widehat{S}_{rn} & -\widehat{v}_{rn} & 0 & \dots & 0 & 0 & 0 \\ 0 & 0 & 0 & \dots & -\widehat{v}_{rn} & \widehat{S}_{rn} & -\widehat{v}_{rn} & \dots & 0 & 0 & 0 \\ 0 & 0 & 0 & \dots & 0 & -\widehat{v}_{rn} & \widehat{S}_{rn} & \dots & 0 & 0 & 0 \\ \dots & \dots & \dots & \dots & \dots & \dots & \dots & \dots & \dots & \dots & .. \\ 0 & 0 & 0 & \dots & 0 & 0 & 0 & \dots & 0 & \widehat{S}_{rn} & -\widehat{v}_{rn} \\ 0 & 0 & 0 & \dots & 0 & 0 & 0 & \dots & 0 & -\widehat{v}_{rn} & \widehat{S}_{rn} \end{bmatrix} \begin{Bmatrix} W_{1rn} \\ W_{2rn} \\ W_{3rn} \\ \dots \\ W_{i-1rn} \\ W_{irn} \\ W_{i+1rn} \\ \dots \\ W_{m-2rn} \\ W_{m-1rn} \\ W_{mrn} \end{Bmatrix} = \begin{Bmatrix} 0 \\ 0 \\ 0 \\ \dots \\ 0 \\ 0 \\ 0 \\ \dots \\ 0 \\ 0 \\ 0 \end{Bmatrix}, \tag{29}$$

where

$$\widehat{S}_{rn} = -\Omega_{rn}^2 f_{rn} - \frac{\delta^2}{12}\Omega_{rn}^2\left(\alpha_r^2 + R^2\beta_n^2\right)f_{rn} + 2\widehat{v}_{rn} + MP\left(\alpha_r^2 - R^2\beta_n^2\right)f_{rn} + (1 + j\Omega_{rn}T_d)\left[\alpha_r^4 + Z_{22}R^4\beta_n^4 + 2(Z_{12} + 2Z_{66})R^2\alpha_r^2\beta_n^2\right], \tag{30a}$$

$$\widehat{v}_{rn} = (K + j\Omega_{rn}B)f_{rn}, \tag{30b}$$

$$f_{rn} = 1 + \eta^2\left(\alpha_r^2 + R^2\beta_n^2\right). \tag{30c}$$

In (Karličić et al., 2016), the methodology of obtaining the analytical solutions for natural frequencies of homogeneous elastic and viscoelastic complex systems is presented. Based on that, we supposed the solution of the *i-th* algebraic equation in (19) as

$$W_{in} = Ncos(i\,\varphi_{cc}) + M\,sin(i\varphi_{cc}), \quad i = 1, 3, \dots, m. \tag{31}$$

Introducing assumed solution (31) into the $i-th$ algebraic equation of the system (29), we obtain two algebraic equations, where constants M and N are not simultaneously equal to zero

$$N\left\{-\widehat{v}_{rn}\,cos[(i-1)\varphi_{cc}] + \widehat{S}_{rn}\,cos(i\,\varphi_{cc}) - \widehat{v}_{rn}\,cos[(i+1)\varphi_{cc}]\right\} = 0, \quad i = 2, 3, \dots, m-1, \tag{32a}$$

$$M\left\{-\widehat{v}_{rn}\,sin[(i-1)\varphi_{cc}] + \widehat{S}_{rn}sin(i\,\varphi_{cc}) - \widehat{v}_{rn}\,sin[(i+1)\varphi_{cc}]\right\} = 0, \quad i = 2, 3, \dots, m-1, \tag{32b}$$

After some algebra we obtain

$$\left(\widehat{S}_{rn} - 2\widehat{v}_{rn}cos\varphi_{cc}\right)Ncos(i\,\varphi_{cc}) = 0, \tag{33a}$$

$$\left(\widehat{S}_{rn} - 2\widehat{v}_{rn}cos\varphi_{cc}\right)Msin(i\,\varphi_{cc}) = 0, \tag{33b}$$

in which, $N \neq 0$ and $cos(i\,\varphi_{cc}) \neq 0$ or $M \neq 0$ and $sin(i\,\varphi_{cc}) \neq 0$ for the case when the system has an oscillatory behavior, for $i = 2, 3, \dots, m-1$. Now, from Eq. (33), we get the complex natural frequency equation of the form

$$\widehat{S}_{rn} = 2\widehat{v}_{rn}cos\varphi_{cc}, \tag{34}$$

where φ_{cc} is unknown parameter determined from the first and the last equation of the system of algebraic equation (29) i.e. from the boundary conditions of the "Clamped −Chain" system.

Using Eq. (21) for the first and for the last equation of the system (29) i.e. $W_{1rn} = Ncos\varphi_{cc} + M\,sin\varphi_{cc}$ and $W_{2rn} = Ncos(2\varphi_{cc}) + M\,sin(2\varphi_{cc})$ into the first equation and $W_{m-1rn} = Ncos[(m-1)\varphi_{cc}] + M\,sin[(m-1)\varphi_{cc}]$ and $W_{m-1rn} = Ncos(m\varphi_{cc}) + M\,sin(m\varphi_{cc})$ into the last equation, we obtain the system of algebraic equations, from which we can find unknown parameter φ_{cc}, as

$$N\left[\widehat{S}_{rn}cos\varphi_{cc} - \widehat{v}_{rn}cos(2\varphi_{cc})\right] + M\left[\widehat{S}_{rn}sin\varphi_{cc} - \widehat{v}_{rn}sin(2\varphi_{cc})\right] = 0, \tag{35a}$$

$$N\left[\widehat{S}_{rn}cos(m\varphi_{cc}) - \widehat{v}_{rn}cos[(m-1)\varphi_{cc}]\right] + M\left[\widehat{S}_{rn}sin(m\varphi_{cc}) - \widehat{v}_{rn}sin[(m-1)\varphi_{cc}]\right] = 0. \tag{35b}$$

Finally, non-trivial solutions of the system of trigonometric equation (35) are

$$\begin{vmatrix} 1 & 0 \\ cos[(m+1)\varphi_{cc}] & sin[(m+1)\varphi_{cc}] \end{vmatrix} = 0 \Rightarrow sin[(m+1)\varphi_{cc}] = 0, \tag{36}$$

from which we have

$$\varphi_{cc,s} = \frac{s\,\pi}{m+1}, \quad s = 1, 2, \dots, m. \tag{37}$$

Substituting expression for $\varphi_{cc,s}$ Eq. (37) into Eq. (34), we obtain the complex natural frequency equation as,

$$-\widehat{a}\Omega_{rn}^2 + j\widehat{b}\Omega_{rn} + \widehat{c} = 0, \quad (r,n) = 1,2,3,\ldots, \tag{38}$$

where

$$\widehat{a} = \left[1 + \frac{\delta^2}{12}\left(\alpha_r^2 + R^2\beta_n^2\right)\right] f_{rn}, \tag{39a}$$

$$\widehat{b} = 2Bf_{rn}(1 - cos\varphi_{cc,s}) + T_d\left[\alpha_r^4 + Z_{22}R^4\beta_n^4 + 2(Z_{12} + 2Z_{66})R^2\alpha_r^2\beta_n^2\right], \tag{39b}$$

$$\widehat{c} = 2Kf_{rn}(1 - cos\varphi_{cc,s}) + MP\left(\alpha_r^2 - R^2\beta_n^2\right)f_{rn} + \left[\alpha_r^4 + Z_{22}R^4\beta_n^4 + 2(Z_{12} + 2Z_{66})R^2\alpha_r^2\beta_n^2\right]. \tag{39c}$$

Solutions of Eq. (38) are complex natural frequencies of VOMNPS given as

$$\Omega_{rncc,s} = +j\frac{\widehat{b}}{2\widehat{a}} \pm \sqrt{\frac{4\widehat{a}\widehat{c} - \widehat{b}^2}{4\widehat{a}^2}}, \quad s = 1,2,\ldots,m, \tag{40}$$

where the imaginary part of Eq. (40) represents damping ratio and the real part represents damped natural frequency.

5.2. "Cantilever - Chain" system

For "Cantilever - Chain" system (Fig. 3) we assume that the first nanoplate is connected to the fixed base through the viscoelastic medium with stiffness coefficient k_0 and damping coefficient b_0 while the last nanoplate in the system is free on the top face where $k_m = 0$ and $b_m = 0$. Therefore, in this case we have the following coupling conditions in the dimensionless form

$$\overline{w}_0(\xi,\zeta,\tau) = 0, \quad \overline{w}_{m+1}(\xi,\zeta,\tau) = 0 \text{ and } K_m = 0, \quad B_m = 0, \tag{41}$$

Substituting coupling conditions (41) and assumed solutions Eq. (26) into Eq. (23), for identical nanoplates and properties of viscoelastic medium between them, we obtain a homogeneous system of m algebraic equations of the form

$$\widehat{S}_{rn}W_{1rn} - \widehat{v}_{rn}W_{2rn} = 0, \quad i = 1, \tag{42a}$$

$$-\widehat{v}_{rn}W_{i-1rn} + \widehat{S}_{rn}W_{irn} - \widehat{v}_{rn}W_{i+1rn} = 0, \quad i = 2,3,..,m-1, \tag{42b}$$

$$-\widehat{v}_{rn}W_{m-1rn} + \left(\widehat{S}_{rn} - \widehat{v}_{rn}\right)W_{mrn} = 0, \quad i = m, \tag{42c}$$

or in the matrix form

$$\begin{bmatrix} \widehat{S}_{rn} & -\widehat{v}_{rn} & 0 & \ldots & 0 & 0 & 0 & \ldots & 0 & 0 & 0 \\ -\widehat{v}_{rn} & \widehat{S}_{rn} & -\widehat{v}_{rn} & \ldots & 0 & 0 & 0 & \ldots & 0 & 0 & 0 \\ \ldots & \ldots & \ldots & \ldots & \ldots & \ldots & \ldots & \ldots & \ldots & \ldots & \ldots \\ 0 & 0 & 0 & \ldots & \widehat{S}_{rn} & -\widehat{v}_{rn} & 0 & \ldots & 0 & 0 & 0 \\ 0 & 0 & 0 & \ldots & -\widehat{v}_{rn} & \widehat{S}_{rn} & -\widehat{v}_{rn} & \ldots & 0 & 0 & 0 \\ 0 & 0 & 0 & \ldots & 0 & -\widehat{v}_{rn} & \widehat{S}_{rn} & \ldots & 0 & 0 & 0 \\ \ldots & \ldots & \ldots & \ldots & \ldots & \ldots & \ldots & \ldots & \ldots & \ldots & .. \\ 0 & 0 & 0 & \ldots & 0 & 0 & 0 & \ldots & 0 & \widehat{S}_{rn} & -\widehat{v}_{rn} \\ 0 & 0 & 0 & \ldots & 0 & 0 & 0 & \ldots & 0 & -\widehat{v}_{rn} & \widehat{S}_{rn} - \widehat{v}_{rn} \end{bmatrix} \begin{Bmatrix} W_{1rn} \\ W_{2rn} \\ W_{3rn} \\ \ldots \\ W_{i-1rn} \\ W_{irn} \\ W_{i+1rn} \\ \ldots \\ W_{m-2rn} \\ W_{m-1rn} \\ W_{mrn} \end{Bmatrix} = \begin{Bmatrix} 0 \\ 0 \\ 0 \\ \ldots \\ 0 \\ 0 \\ 0 \\ \ldots \\ 0 \\ 0 \\ 0 \end{Bmatrix}, \tag{43}$$

where $\widehat{S}_{rn}$ and $-\widehat{v}_{rn}$ are defined in Eq. (30).

Applying Eq. (31) into the $i-th$ algebraic equation of the system (43), we obtain the same two trigonometric expressions as in the previous case, which leads to a complex natural frequency equation $\widehat{S}_{rn} = 2\widehat{v}_{rn}cos\varphi_{can}$. Different chain conditions of coupling for the first and the last nanoplate in VOMNPS with a fixed base leads to a change in the system of algebraic equation (43). Therefore, it is necessary to find new value of unknown parameter φ_{can} from the first and the last equation of the system (43). Introducing $W_{1n} = Ncos\varphi_{can} + M\,sin\varphi_{can}$ and $W_{2n} = Ncos(2\varphi_{can}) + M\,sin(2\varphi_{can})$ into the first equation and $W_{m-1n} = Ncos[(m-1)\varphi_{can}] + M\,sin[(m-1)\varphi_{can}]$ and $W_{m-1n} = Ncos(m\varphi_{can}) + M\,sin(m\varphi_{can})$

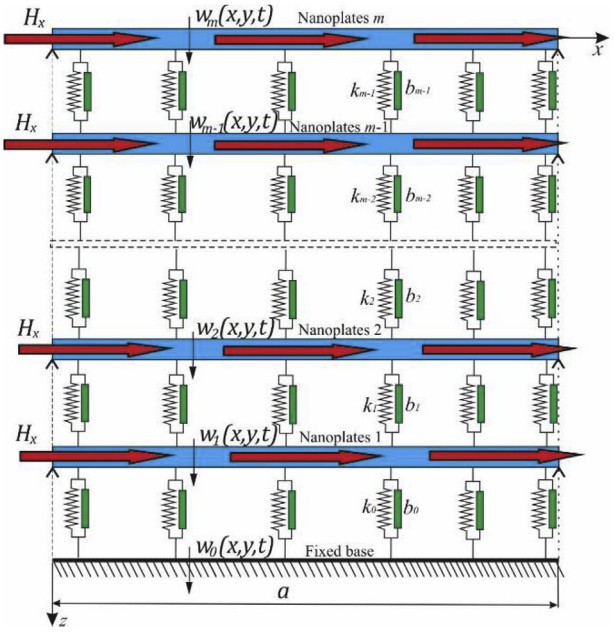

Fig. 3. Side view of VOMNPS embedded in the viscoelastic medium and under the influence of uniaxial in-plane magnetic force, "Cantilever-Chain" systems.

into the last equation of (43), we obtain the new system of algebraic equations as

$$N[S_{rn}cos\varphi_{can} - v_{rn}cos(2\varphi_{can})] + M[S_n sin\varphi_{cc} - v_{rn}sin(2\varphi_{can})] = 0, \tag{44a}$$

$$N[(S_{rn} - v_n)cos(m\varphi_{can}) - v_{rn}cos[(m-1)\varphi_{can}]] + M[(S_{rn} - v_{rn})sin(m\varphi_{can}) - v_{rn}sin[(m-1)\varphi_{can}]] = 0. \tag{44b}$$

The non-trivial solutions for constants N and M are obtained from the above system, which yields the following trigonometric relation

$$N[(S_{rn} - v_n)cos(m\varphi_{can}) - v_{rn}cos[(m-1)\varphi_{can}]] + M[(S_{rn} - v_{rn})sin(m\varphi_{can}) - v_{rn}sin[(m-1)\varphi_{can}]] = 0. \tag{44c}$$

where unknown $\varphi_{can,s}$ is obtained for the "Cantilever-Chain" system as

$$\varphi_{can,s} = \frac{(2s-1)\,\pi}{2m+1}, \quad s = 1, 2, \ldots, m. \tag{46}$$

Introducing the parameter $\varphi_{can,s}$ into Eq. (34) instead of φ_{cc}, the complex natural frequency equation is obtained as in the previous case

$$-\widehat{a}\Omega_{rn}^2 + j\widehat{b}\Omega_{rn} + \widehat{c} = 0, (r,n) = 1, 2, 3, \ldots, \tag{47}$$

The solution of Eq. (47) represents the complex natural frequency of VOMNPS of the form

$$\Omega_{rncan,s} = +j\frac{\widehat{b}}{2\widehat{a}} \pm \sqrt{\frac{4\widehat{a}\widehat{c} - \widehat{b}^2}{4\widehat{a}^2}}, \quad s = 1, 2, \ldots, m. \tag{49}$$

5.3. "Free-Chain" system

Next, we consider the system where the first and the last nanoplate are without coupling with the fixed base, where coupling conditions in dimensionless form are

$$K_0 = 0, \; K_m = 0 \quad \text{and} \quad B_0 = 0, \; B_m = 0, \tag{50}$$

Using the chain coupling conditions for the "Free-Chain" system (Fig. 4) Eq. (50) and assumed solution (26), from the equation of motion Eq. (23) we obtain the following system of algebraic equations

$$\left(\widehat{S}_{rn} - \widehat{v}_{rn}\right)W_{1rn} - \widehat{v}_{rn}W_{2rn} = 0, \quad i = 1, \tag{51a}$$

$$-\widehat{v}_{rn}W_{i-1rn} + \widehat{S}_{rn}W_{irn} - \widehat{v}_{rn}W_{i+1rn} = 0, \quad i = 2, 3, .., m-1, \tag{51b}$$

$$-\widehat{v}_{rn}W_{m-1rn} + \left(\widehat{S}_{rn} - \widehat{v}_{rn}\right)W_{mrn} = 0, \quad i = m, \tag{51c}$$

or in the matrix form

$$\begin{bmatrix} \widehat{S}_{rn}-\widehat{v}_{rn} & -\widehat{v}_{rn} & 0 & \ldots & 0 & 0 & 0 & \ldots & 0 & 0 & 0 \\ -\widehat{v}_{rn} & \widehat{S}_{rn} & -\widehat{v}_{rn} & \ldots & 0 & 0 & 0 & \ldots & 0 & 0 & 0 \\ \ldots & \ldots & \ldots & \ldots & \ldots & \ldots & \ldots & \ldots & \ldots & \ldots & \ldots \\ 0 & 0 & 0 & \ldots & \widehat{S}_{rn} & -\widehat{v}_{rn} & 0 & \ldots & 0 & 0 & 0 \\ 0 & 0 & 0 & \ldots & -\widehat{v}_{rn} & \widehat{S}_{rn} & -\widehat{v}_{rn} & \ldots & 0 & 0 & 0 \\ 0 & 0 & 0 & \ldots & 0 & -\widehat{v}_{rn} & \widehat{S}_{rn} & \ldots & 0 & 0 & 0 \\ \ldots & \ldots & \ldots & \ldots & \ldots & \ldots & \ldots & \ldots & \ldots & \ldots & .. \\ 0 & 0 & 0 & \ldots & 0 & 0 & 0 & \ldots & 0 & \widehat{S}_{rn} & -\widehat{v}_{rn} \\ 0 & 0 & 0 & \ldots & 0 & 0 & 0 & \ldots & 0 & -\widehat{v}_{rn} & \widehat{S}_{rn}-\widehat{v}_{rn} \end{bmatrix} \begin{Bmatrix} W_{1rn} \\ W_{2rn} \\ W_{3rn} \\ \ldots \\ W_{i-1rn} \\ W_{irn} \\ W_{i+1rn} \\ \ldots \\ W_{m-2rn} \\ W_{m-1rn} \\ W_{mrn} \end{Bmatrix} = \begin{Bmatrix} 0 \\ 0 \\ 0 \\ \ldots \\ 0 \\ 0 \\ 0 \\ \ldots \\ 0 \\ 0 \\ 0 \end{Bmatrix}, \tag{52}$$

where the only difference is in the parameter $\varphi_{can,s}$ and

$$\widehat{a} = \left[1 + \frac{\delta^2}{12}\left(\alpha_r^2 + R^2\beta_n^2\right)\right]f_{rn}, \tag{48a}$$

$$\widehat{b} = 2Bf_{rn}(1 - cos\varphi_{can,s}) + T_d\left[\alpha_r^4 + Z_{22}R^4\beta_n^4 + 2(Z_{12} + 2Z_{66})R^2\alpha_r^2\beta_n^2\right], \tag{48b}$$

$$\widehat{c} = 2Kf_{rn}(1 - cos\varphi_{can,s}) + MP\left(\alpha_r^2 - R^2\beta_n^2\right)f_{rn} + \left[\alpha_r^4 + Z_{22}R^4\beta_n^4 + 2(Z_{12} + 2Z_{66})R^2\alpha_r^2\beta_n^2\right]. \tag{48c}$$

where expressions $\widehat{S}_{rn}$ and $\widehat{v}_{rn}$ are defined in Eq. (30).

By using assumed solution Eq. (31) into $i-th$ algebraic equation of the system (52), we get the complex natural frequency equation in the same way as in the previous cases. We have that $\widehat{S}_{rn} = 2\widehat{v}_{rn}cos\varphi_{fc}$, where φ_{fc} is unknown parameter determined from the first and the last equation of the system of algebraic equation (52) i.e. boundary conditions of the "Free-Chain" system. Applying solutions for the first and the second amplitude, $W_{1rn} = Ncos\varphi_{fc} + M\,sin\varphi_{fc}$ and $W_{2rn} = Ncos(2\varphi_{fc}) + M\,sin(2\varphi_{fc})$, into the first equation and $W_{m-1n} = Ncos[(m-1)\varphi_{fc}] + M\,sin[(m-1)\varphi_{fc}]$ and $W_{m-1n} = Ncos(m\varphi_{fc}) + M\,sin(m\varphi_{fc})$ into the last equation of system (52), and after some algebra we obtain

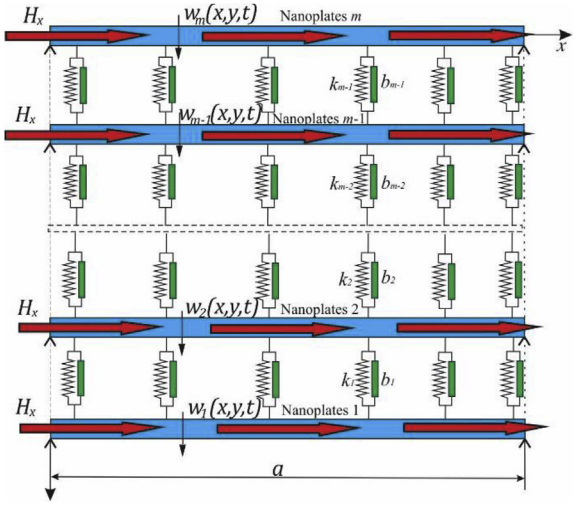

Fig. 4. Side view of VOMNPS embedded in the viscoelastic medium and under the influence of uniaxial in-plane magnetic force, "Free-Chain" systems.

$$N\left[\left(\widehat{S}_{rn}-\widehat{v}_{rn}\right)cos\varphi_{fc}-\widehat{v}_{rn}cos\left(2\varphi_{fc}\right)\right]+M\left[\left(\widehat{S}_{rn}-\widehat{v}_{rn}\right)sin\varphi_{fc}-\widehat{v}_{rn}sin\left(2\varphi_{fc}\right)\right]=0, \tag{53a}$$

$$N\left[\left(\widehat{S}_{rn}-\widehat{v}_{rn}\right)cos\left(m\varphi_{fc}\right)-\widehat{v}_{rn}cos\left[(m-1)\varphi_{fc}\right]\right]+M\left[\left(\widehat{S}_{rn}-\widehat{v}_{rn}\right)sin\left(m\varphi_{fc}\right)-\widehat{v}_{rn}sin\left[(m-1)\varphi_{fc}\right]\right]=0. \tag{53b}$$

where the non-trivial solution leads to the trigonometric equations in the following form

$$\begin{vmatrix} 1-cos\varphi_{fc} & -sin\varphi_{fc} \\ cos[(m+1)\varphi_{cc}]-cos\left(m\varphi_{fc}\right) & sin[(m+1)\varphi_{cc}]-sin\left(m\varphi_{fc}\right) \end{vmatrix} = 0 \Rightarrow sin\left(m\varphi_{fc}\right)=0, \tag{54}$$

where unknown $\varphi_{fc,s}$ is equal to

$$\varphi_{fc,s}=\frac{s\,\pi}{m},\quad s=0,1,\ldots,m-1. \tag{55}$$

Introducing the parameter $\varphi_{fc,s}$ into Eq. (34) instead of φ_{cc}, the complex natural frequency equation is obtained as

$$-\widehat{a}\Omega_{rn}^2+j\widehat{b}\Omega_{rn}+\widehat{c}=0,(r,n)=1,2,3,\ldots, \tag{56}$$

where the only difference is in the parameter $\varphi_{fc,s}$ and

$$\widehat{a}=\left[1+\frac{\delta^2}{12}\left(\alpha_r^2+R^2\beta_n^2\right)\right]f_{rn}, \tag{57a}$$

$$\widehat{b}=2Bf_{rn}\left(1-cos\varphi_{fc,s}\right)+T_d\left[\alpha_r^4+Z_{22}R^4\beta_n^4+2(Z_{12}+2Z_{66})R^2\alpha_r^2\beta_n^2\right], \tag{57b}$$

$$\widehat{c}=2Kf_{rn}\left(1-cos\varphi_{fc,s}\right)+MP\left(\alpha_r^2-R^2\beta_n^2\right)f_{rn}+\left[\alpha_r^4+Z_{22}R^4\beta_n^4+2(Z_{12}+2Z_{66})R^2\alpha_r^2\beta_n^2\right]. \tag{57c}$$

Finally, the solution of Eq. (56) represents the complex natural frequency of VOMNPS in the form

$$\Omega_{rnfc,s}=+j\frac{\widehat{b}}{2\widehat{a}}\pm\sqrt{\frac{4\widehat{a}\widehat{c}-\widehat{b}^2}{4\widehat{a}^2}},\quad s=1,2,\ldots,m. \tag{58}$$

5.4. Asymptotic values of complex natural frequency

Here, we consider the case when a number of viscoelastic orthotropic nanoplates tends to infinity i.e. we introduce $m\to\infty$ into the expressions for complex natural frequency (40), (49) and (58). Since the expressions for the parameter φ are equal to zero in all cases$(\varphi_{cc,s},\varphi_{can,s},\varphi_{fc,s})=0$, we conclude that there is an independent critical value of the complex natural frequency, also called fundamental complex natural frequency, regardless to the chain coupling conditions, defined as

$$\underset{m\to\infty}{\Omega_{rn}}=\mathrm{Im}\left[\underset{m\to\infty}{\Omega_{rn}}\right]j\pm\mathrm{Re}\left[\underset{m\to\infty}{\Omega_{rn}}\right],\quad (r,n)=1,2,\ldots, \tag{59}$$

where

$$\mathrm{Im}\left[\underset{m\to\infty}{\Omega_{rn}}\right]=\frac{\overline{\overline{b}}}{2\widehat{a}},\quad \text{and}\quad \mathrm{Re}\left[\underset{m\to\infty}{\Omega_{rn}}\right]=\sqrt{\frac{4\widehat{a}\overline{\overline{c}}-\overline{\overline{b}}^2}{4\widehat{a}^2}}, \tag{60a}$$

$$\widehat{a}=\left[1+\frac{\delta^2}{12}\left(\alpha_r^2+R^2\beta_n^2\right)\right]f_{rn}, \tag{60b}$$

$$\overline{\overline{b}}=T_d\left[\alpha_r^4+Z_{22}R^4\beta_n^4+2(Z_{12}+2Z_{66})R^2\alpha_r^2\beta_n^2\right], \tag{60c}$$

$$\overline{\overline{c}}=MP\left(\alpha_r^2-R^2\beta_n^2\right)f_{rn}+\left[\alpha_r^4+Z_{22}R^4\beta_n^4+2(Z_{12}+2Z_{66})R^2\alpha_r^2\beta_n^2\right], \tag{60d}$$

The real parts of complex natural frequencies represent the critical damped natural frequencies of VOMNPS, while imaginary parts of complex natural frequencies represent the critical damped ratios. In the case when the real parts of critical complex natural frequencies are equal to zero, we can obtain the critical values of internal damping as

$$\mathrm{Re}\left[\underset{m\to\infty}{\Omega_{rn}}\right]=0,\Rightarrow(T_d)_{\underset{m\to\infty}{cr}}=\frac{\sqrt{4\left[1+\frac{\vartheta^2}{12}\left(\alpha_r^2+R^2\beta_n^2\right)\right]f_{rn}\left[MP\left(\alpha_r^2-R^2\beta_n^2\right)f_{rn}+\alpha_r^4+Z_{22}R^4\beta_n^4+2(Z_{12}+2Z_{66})R^2\alpha_r^2\beta_n^2\right]}}{\left[\alpha_r^4+Z_{22}R^4\beta_n^4+2(Z_{12}+2Z_{66})R^2\alpha_r^2\beta_n^2\right]},\tag{61}$$

It should be noted that both parts of critical complex natural frequencies are functions of nanoplates material parameters and are independent of a number of nanoplates, chain coupling conditions and influences of the viscoelastic medium.

6. Validation and numerical results

In this section, we validate our results for complex natural frequencies by solving the systems of algebraic equations (29) (43) and (52) analytically using the trigonometric method and numerically using the corresponding function in Wolfram Mathematica software. In addition, a detailed parametric study is conducted by investigating the effects of dimensionless nonlocal parameter, internal viscosity, magnetic field parameter and aspect ratios on dimensionless real and imaginary parts of complex natural frequency. Obtained results are discussed and some conclusions are made.

6.1. Validation of the results

In order to illustrate the accuracy of the proposed trigonometric method, we performed numerical simulations for three and five nanoplates in simply supported VOMNPS embedded in viscoelastic medium and for three different chain conditions “Clamped-Chain”, “Cantilever-Chain” and “Free-Chain”. By browsing the literature, the authors have found that some researchers (Behfar and Naghdabadi, 2005; Arghavan, 2012; Pradhan and Kumar, 2011; Ni et al., 2010; Pradhan and Phadikar, 2009; Shen et al., 2010, 2011), based on different approaches (molecular dynamic simulation, lattice structure, nonlocal continuum mechanics), investigated elastic properties of a single layer graphene sheet. They obtained two values of Young elastic modulus for two perpendicular/orthogonal directions, i.e. in that case the graphene sheet can be considered as orthotropic plate (Reddy, 2006). Based on that fact, the authors adopted continuum model for a single layer graphene sheet as thin orthotropic plate, where size effects are introduced through Eringen's nonlocal elasticity theory. Moreover, in the present work we investigate the system of multiple graphene sheets embedded in polymer matrix as a system of multiple viscoelastically coupled orthotropic nanoplates, where such model is more general than using the isotropic nanoplate model. However, present model can be easily modified to investigate a system of isotropic nanoplates only by using the following assumptions $E_1 = E_2 = E$ and $\vartheta_{12} = \vartheta_{21} = \vartheta$.

In given numerical examples, the following values of parameters are adopted: length $a = 9.519[nm]$ and width $b = 4.844[nm]$, elastic modules of orthotropic nanoplates as $E_1 = 2.434[TPa]$ and$E_2 = 2.473[TPa]$, Poisson's ratios $\vartheta_{12} = \vartheta_{21} = 0.197$, thickness of nanoplates $h = 0.129[nm]$ and mass density $\rho = 6316[kg/m^3]$, (Shen et al., 2010, 2011). The coefficients of viscoelastic media, magnetic field parameter and internal damping coefficient are considered as dimensionless parameters $K = 100, B = 10,\ MP = 10$ and$T = 0.01$. These material and geometric parameters for orthotropic viscoelastic nanoplates are adopted from the paper (Pouresmaeeli et al., 2013).

One can notice an excellent agreement between the results obtained from the analytical and the numerical method (Table 1). Further, it can be noticed that the highest complex natural frequency in the “Clamped-Chain” system is the same and does not depend on the number of nanoplates in VOMNPS. The lowest value of the complex natural frequency, determined for$s = 1$, decreases with an increase of the number of nanoplates. In the case of “Cantilever-Chain” system, the highest complex natural frequency increases while the lowest one (also for$s = 1$) decreases for an increase of the number of nanoplates in VOMNPS. Finally, for the case of “Free-Chain” system, the lowest complex natural frequency determined for $s = 0$ is the same while the highest one increases for an increase of the number of nanoplates in VOMNPS. The lowest value of complex natural frequency in the last case is equivalent to the fundamental complex natural frequency of the system obtained from asymptotic analysis when the number of nanoplates tends to infinity.

6.2. Parametric study

We must note that all values of parameters used in the following simulations are same as in the previous case except those parameters that are varied to examine its effect on complex natural frequencies. Fig. 5 illustrates the effects of internal viscosity T_d and

Table 1
Validation of dimensionless damped natural frequencies $\Omega_{11,s}$ of VOMNPS for three chain systems and varying number of nanoplates.

r = 1 n = 1		Clamped-Chain		Cantilever-Chain		Free-Chain	
		Trig. method Eq. (40)	Num. method Eq. (29)	Trig. method Eq. (49)	Num. method Eq. (43)	Trig. method Eq. (58)	Num. method Eq. (52)
m = 3	1	10.2543 + 17.4012 I	10.2543 + 17.4012 I	9.19994 + 1.32308 I	9.19994 + 1.32308 I	8.15325 + 0.33293 I	8.15325 + 0.33293 I
	2	10.7013 + 3.26138 I	10.7013 + 3.26138 I	10.8086 + 16.5652 I	10.8086 + 16.5652 I	11.4680 + 15.3305 I	11.4680 + 15.3305 I
	3	12.6419 + 10.3313 I	12.6419 + 10.3313 I	12.5037 + 8.10644 I	12.5037 + 8.10644 I	11.7532 + 5.33211 I	11.7532 + 5.33211 I
m = 5	1	8.89413 + 18.9901 I	8.89413 + 18.9901 I	8.61057 + 0.73793 I	8.61057 + 0.73793 I	8.15325 + 0.33293 I	8.15325 + 0.33293 I
	2	9.51734 + 1.67246 I	9.51734 + 1.67246 I	9.13770 + 18.7424 I	9.13770 + 18.7424 I	9.43553 + 18.4201 I	9.43553 + 18.4201 I
	3	11.4680 + 15.3305 I	11.4680 + 15.3305 I	11.0130 + 3.78376 I	11.0130 + 3.78376 I	9.98740 + 2.24245 I	9.98740 + 2.24245 I
	4	11.7532 + 5.33211 I	11.7532 + 5.33211 I	11.8243 + 14.4848 I	11.8243 + 14.4848 I	12.1748 + 13.4209 I	12.1748 + 13.4209 I
	5	12.6419 + 10.3313 I	12.6419 + 10.3313 I	12.5991 + 8.90837 I	12.5991 + 8.90837 I	12.3418 + 7.24163 I	12.3418 + 7.24163 I

* $I = \sqrt{-1}$ –imaginary unit.

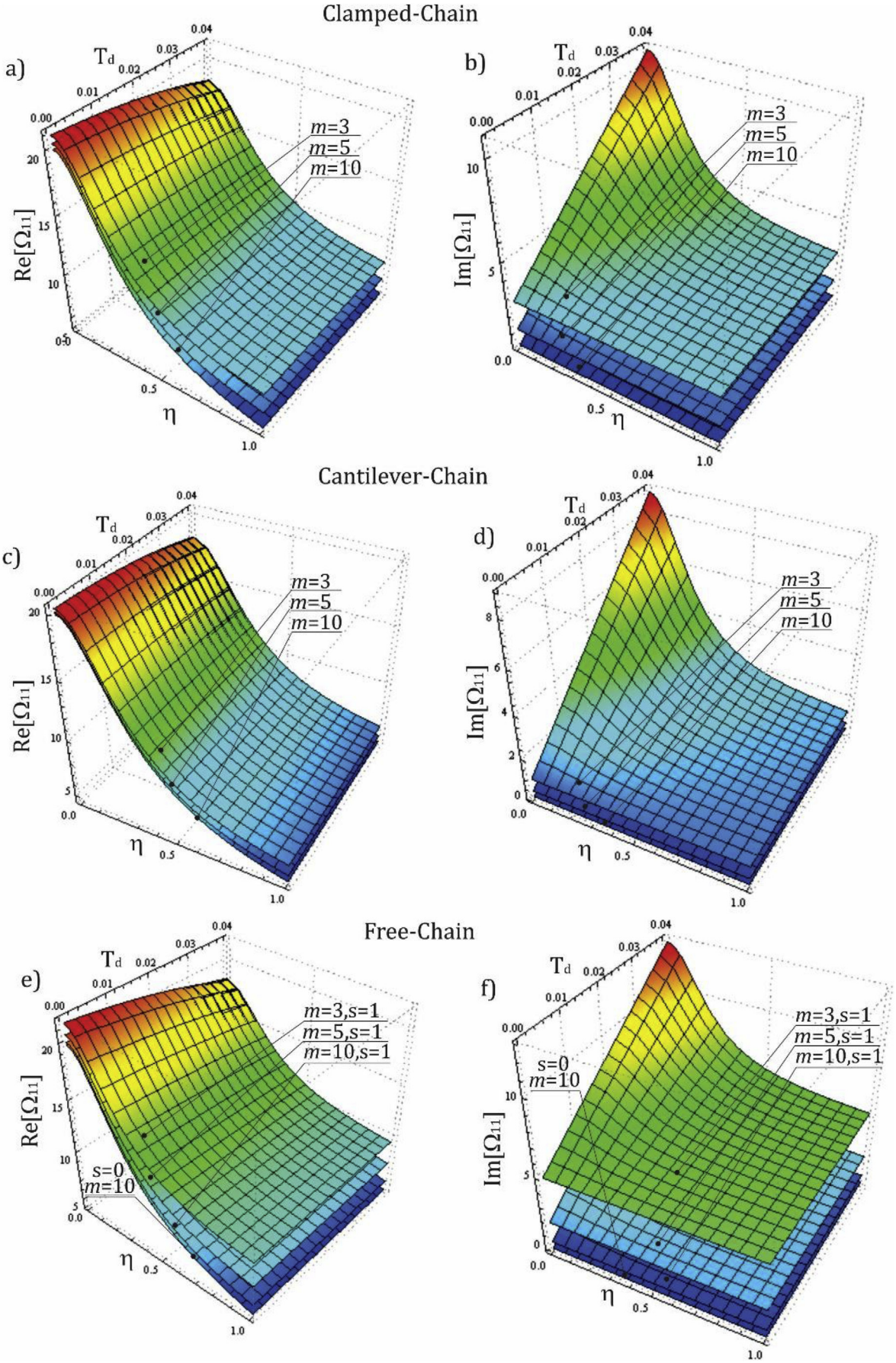

Fig. 5. Effects of nonlocal η and internal viscosity T_d parameters on complex natural frequency of VOMNPS.

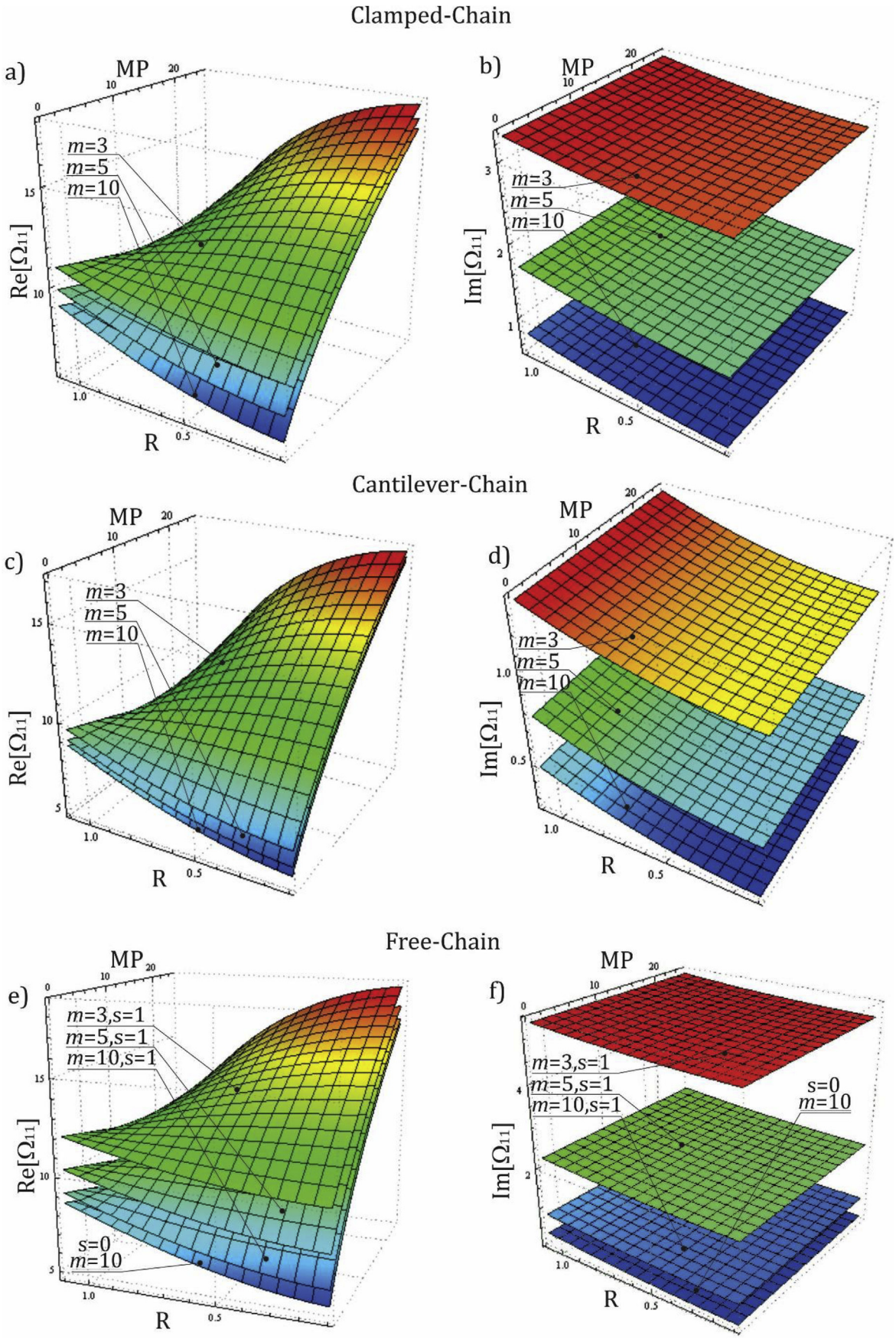

Fig. 6. Effects of magnetic field parameter MP and aspect ratio R on complex natural frequency of VOMNPS.

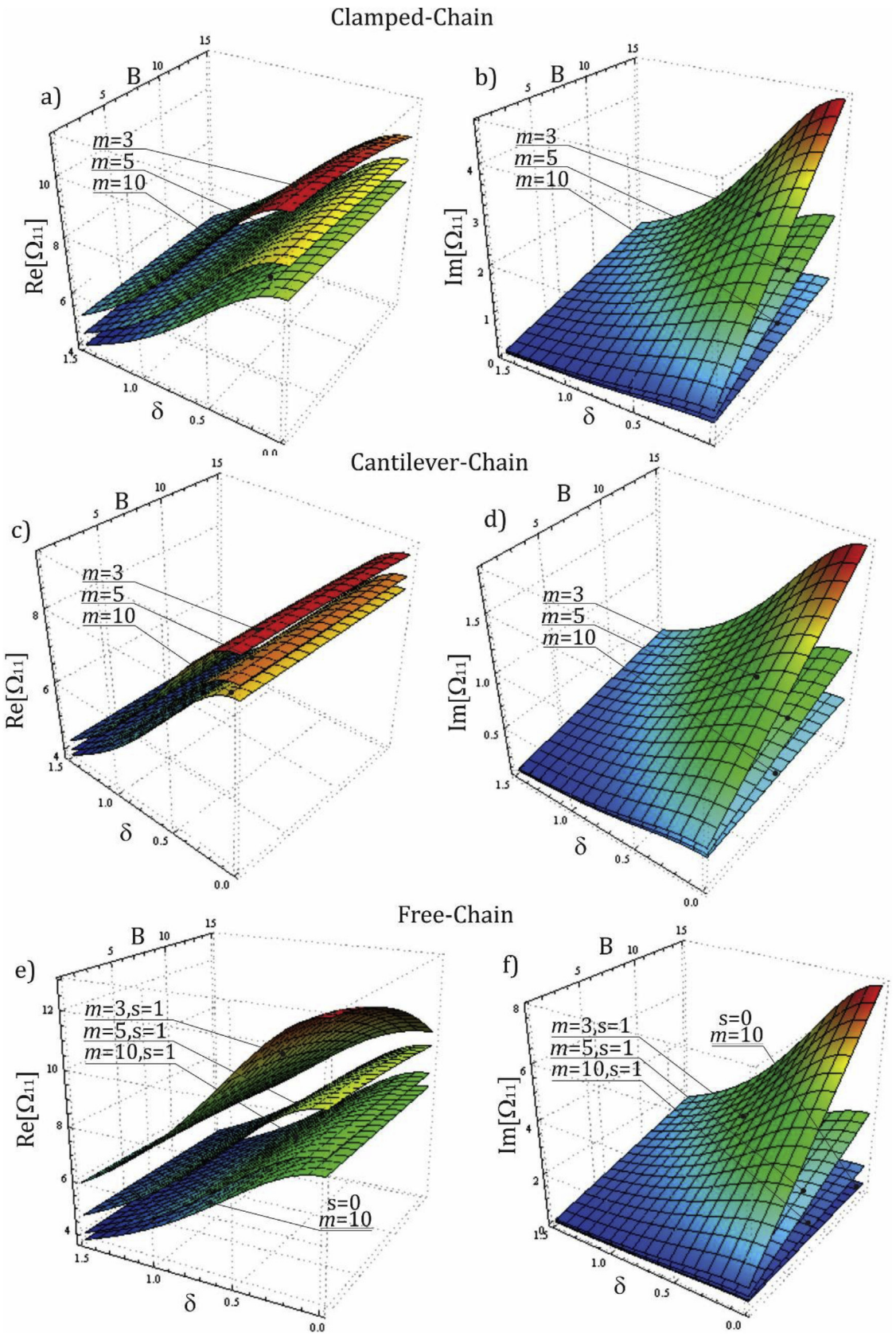

Fig. 7. Effects of damping coefficient of the viscoelastic medium B and aspect ratio δ on complex natural frequency of VOMNPS.

nonlocal parameter η on the real and imaginary parts of the lowest complex natural frequency for different number of nanoplates in VOMNPS. In the case of "Clamped-Chain" system, it can be observed that the real part of complex natural frequency i.e. damped natural frequency decreases significantly for an increase of nonlocal parameter. The imaginary i.e. damping ratio part of the complex natural frequency increases significantly for an increase of the internal viscosity and it decreases for an increase of the nonlocal parameter. In the case of "Cantilever-Chain" system, the real and the imaginary part of complex natural frequency decreases for an increase of the nonlocal parameter. In addition, the real part of complex natural frequency slightly decreases whereas the imaginary part increases for an increase of internal viscosity. The same influence of internal viscosity and nonlocal parameter can be recognized in the case of "Free-Chain" system. An increase of nonlocal parameter decreases complex natural frequency whereas an increase of internal viscosity decreases the real part of frequency and increases the imaginary part. However, for the last chain conditions the lowest complex frequency is the same for different numbers of nanoplates in VOMNPS and it is obtained for $s = 0$. Thus, we conclude that the lowest frequency is in fact the fundamental complex natural frequency. Therefore, on the same figure we plotted the complex natural frequency of "Free-Chain" system for $s = 1$ and observed that for a significant increase of a number of nanoplates complex frequency tends to the fundamental frequency, which is in line with the asymptotic analysis. Next, the common conclusion is that the complex natural frequency decreases for an increase of a number of nanoplates in VOMNPS.

In Fig. 6, the real and imaginary part of complex natural frequency are plotted for changes of magnetic field parameter MP and aspect ratio R and other parameters same as in Table 1. One can notice that when no or weak magnetic field is applied to VOMNPS, the real part of complex natural frequency increases for an increase of aspect ratio starting from low values of frequency. However, for applied stronger magnetic field the real part of complex natural frequency decreases significantly for an increase of aspect ratio R starting from much higher values of frequency. This effect can be recognized for all three cases of chain conditions. In addition, for the "Clamped-Chain" and "Free-Chain" systems the imaginary part of complex natural frequency slightly increases for an increase of aspect ratio whereas it is constant for changes of magnetic field parameter. In the "Cantilever-Chain" system, an increase of the imaginary part of complex natural frequency for an increase of aspect ratio is more pronounced than in the previous two cases while the frequency is constant for changes of magnetic field parameter. Further, in all three cases of chain conditions the value of complex natural frequency decreases for an increase of a number of nanoplates in VOMNPS.

Next, we illustrate the influence of aspect ratio δ and damping coefficient B of the viscoelastic medium on the complex natural frequency of VOMNPS. The values of other parameters are same as in the previous cases. In Fig. 7, it can be noticed that an increase of damping coefficient almost has no visible effects on the real part of complex natural frequency except for the slight decrease of frequency for lower number of nanoplates in VOMNPS, especially in the case of "Free-Chain" system. The imaginary part of complex natural frequency increases for an increase of damping coefficient for all cases of chain conditions. The effect of increase of aspect ratio δ is a decrease of complex natural frequency. In general, an increase of a number of nanoplates in VOMNPS decreases the complex natural frequency.

Further, we show the influence of nonlocal parameter, different chain conditions and significant change of a number of nanoplates in VOMNPS on the real and imaginary part of the lowest complex natural frequency. As stated before, from Fig. 8 it is obvious that an increase of nonlocal parameter decreases both parts of complex natural frequency. For results in Table 1 we mentioned that the lowest frequency of "Free-Chain" system is for $s = 0$ and it is equal to the fundamental frequency of the system obtained from asymptotic analysis. In the case of "Clamped-Chain" and "Cantilever-Chain" systems, the lowest frequency is obtained for $s = 1$. For curves of "Clamped-Chain" and "Cantilever-Chain" it can be noticed that they are approaching to the curve of the lowest complex natural frequency of "Free-Chain" system i.e. the fundamental frequency, for an increase of the number of nanoplates in VOMNPS.

From the detailed parametric study, it can be noticed that the influence of magnetic parameter on the real part of complex natural frequency i.e. the damped natural frequency of VOMNPS is significant. However, an increase of aspect ratio by increasing the length or height of nanoplate in the direction of magnetic field can reduce its influence on the real part of complex natural frequency of the system dramatically. This effect is also recognized in theoretical studies analyzing the vibration behavior of CNTs with applied magnetic field in the direction of the length of nanotube. The results presented in this study may be significant for the future investigations of complex nanostructure systems exploited in the presence of magnetic field.

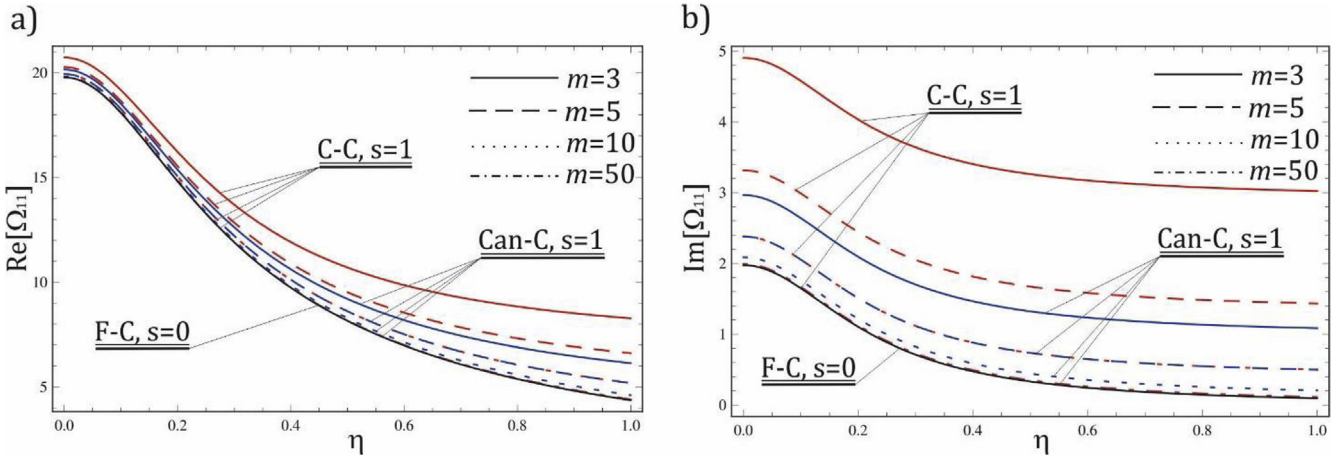

Fig. 8. Effect of increase of the number of nanoplates on complex natural frequency of VOMNPS with different chain conditions.

7. Conclusion

In this paper, we summarized current advances in the field of theoretical analysis of mechanical behavior of complex nanostructure systems such as nanoplate-like structures in the presence of magnetic field. Further, we performed the free vibration study of VOMNPS embedded in the viscoelastic medium and under the influence of in-plane magnetic field by using nonlocal theory. Explicit equations for complex natural frequencies are determined via trigonometric method. In addition, by performing the asymptotic analysis we determined critical values of complex natural frequency and internal damping. From obtained numerical results, characteristic behaviors of complex natural frequencies are identified for changes of nonlocal parameter, internal damping parameter, magnitude of a magnetic field, damping coefficient of the layers and different numbers of nanoplates in VOMNPS. The results revealed that the influence of magnetic field on the real part of complex natural frequency is significant but it strongly depends on the dimension of a nanostructure in the direction of magnetic field i.e. an increase of aspect ratio decreases the influence of magnetic field parameter. The methods used in this work can be useful for the future vibration studies of complex nanostructure systems that consider models with included influence of different physical fields.

Acknowledgments

This research was supported by the research grant of the Serbian Ministry of Science and Environmental Protection under the numbers ON 174001 and ON 174011.

References

Ahir, S.V., Huang, Y.Y., Terentjev, E.M., 2008. Polymers with aligned carbon nanotubes: active composite materials. Polymer 49, 3841–3854.
Ansari, R., Sahmani, S., Arash, B., 2010. Nonlocal plate model for free vibrations of single-layered graphene sheets. Phys. Lett. A 375 (1), 53–62.
Ansari, R., Arash, B., Rouhi, H., 2011. Vibration characteristics of embedded multi-layered graphene sheets with different boundary conditions via nonlocal elasticity. Compos. Struct. 93 (9), 2419–2429.
Arani, A.G., Maboudi, M.J., Arani, A.G., Amir, S., 2013. 2D-Magnetic field and biaxiall in-plane pre-load effects on the vibration of double bonded orthotropic graphene sheets. J. Solid Mech. 5 (2), 193–205.
Arani, A.G., Maboudi, M.J., Kolahchi, R., 2014. Nonlinear vibration analysis of visoelastically coupled DLAGS-systems. Eur. J. Mech. A Solids 45, 185–197.
Arash, B., Wang, Q., 2014. A Review on the Application of Nonlocal Elastic Models in Modeling of Carbon Nanotubes and Graphenes. In Modeling of Carbon Nanotubes, Graphene and Their Composites. Springer International Publishing, pp. 57–82.
Arghavan, S., 2012. Vibration of Carbon Nano-structures. Doctoral dissertation. The University of Western Ontario.
Behfar, K., Naghdabadi, R., 2005. Nanoscale vibrational analysis of a multi-layered graphene sheet embedded in an elastic medium. Compos. Sci. Technol. 65 (7), 1159–1164.
Bunch, J.S., Van Der Zande, A.M., Verbridge, S.S., Frank, I.W., Tanenbaum, D.M., Parpia, J.M., et al., 2007. Electromechanical resonators from graphene sheets. Science 315 (5811), 490–493.
Camponeschi, E., Vance, R., Al-Haik, M., Garmestani, H., Tannenbaum, R., 2007. Properties of carbon nanotube–polymer composites aligned in a magnetic field. Carbon 45 (10), 2037–2046.
Eringen, A.C., 1972. Linear theory of nonlocal elasticity and dispersion of plane waves. Int. J. Eng. Sci. 10 (5), 425–435.
Eringen, A.C., 1983. On differential equations of nonlocal elasticity and solutions of screw dislocation and surface waves. J. Appl. Phys. 54 (9), 4703–4710.
Faugeras C, Kossacki P, Basko D, Amado M, Sprinkle M, Berger C, et al. Effect of a magnetic field on the two-phonon Raman scattering in graphene. Phys. Rev. B2010:81.
Fu, Z., Wang, Z., Li, S., Zhang, P., 2011. Magnetic quantum oscillations in a monolayer graphene under a perpendicular magnetic field. Chin. Phys. B 20.
Fujiwara, M., Oki, E., Hamada, M., Tanimoto, Y., Mukouda, I., Shimomura, Y., 2001. Magnetic orientation and magnetic properties of a single carbon nanotube. J. Phys. Chem. A 105 (18), 4383–4386.
Garmestani, H., Al-Haik, M.S., Dahmen, K., Tannenbaum, R., Li, D., Sablin, S.S., Hussaini, M.Y., 2003. Polymer-mediated alignment of carbon nanotubes under high magnetic fields. Adv. Mater. 15 (22), 1918–1921.
Golberg, D., Bando, Y., Huang, Y., Terao, T., Mitome, M., Tang, C., Zhi, C., 2010. Boron nitride nanotubes and nanosheets. ACS Nano 4 (6), 2979–2993.
Grimes, C.A., Mungle, C., Kouzoudis, D., Fang, S., Eklund, P.C., 2000. The 500 MHz to 5.50 GHz complex permittivity spectra of single-wall carbon nanotube-loaded polymer composites. Chem. Phys. Lett. 319, 460–464.
Hao, F., Fang, D., Xu, Z., 2011. Mechanical and thermal transport properties of graphene with defects. Appl. Phys. Lett. 99 (4), 041901.
Huu-Tai, T., 2012. A nonlocal beam theory for bending, buckling, and vibration of nanobeams. Int. J. Eng. Sci. 52, 56–64.
Kan, E., Li, Z., Yang, J., 2008. Magnetism in graphene systems. Nano 3 (06), 433–442.
Karličić, D., Murmu, T., Adhikari, S., McCarthy, M., 2016. Non-local Structural Mechanics. Wiley-ISTE, London.
Kiani, K., 2014. Vibration and instability of a single-walled carbon nanotube in a three-dimensional magnetic field. J. Phys. Chem. Solids 75 (1), 15–22.
Kiani, K., 2014. Free vibration of conducting nanoplates exposed to unidirectional in-plane magnetic fields using nonlocal shear deformable plate theories. Phys. E Low-dimensional Syst. Nanostruct. 57, 179–192.
Kiani, K., 2014. Revisiting the free transverse vibration of embedded single-layer graphene sheets acted upon by an in-plane magnetic field. J. Mech. Sci. Technol. 28 (9), 3511–3516.
Kimura, T., Ago, H., Tobita, M., Ohshima, S., Kyotani, M., Yumura, M., 2002. Polymer composites of carbon nanotubes aligned by a magnetic field. Adv. Mater. 14, 1380–1383.
Kröner, E., 1967. Elasticity theory of materials with long range cohesive forces. Int. J. Solids Struct. 3 (5), 731–742.
Li, N., Wang, Z., Zhao, K., Shi, Z., Gu, Z., Xu, S., 2010. Large scale synthesis of N-doped multi-layered graphene sheets by simple arc-discharge method. Carbon 48 (1), 255–259.
Liang, Y., Han, Q., 2014. Prediction of the nonlocal scaling parameter for graphene sheet. Eur. J. Mech. A Solids 45, 153–160.
Lin, R.M., 2012. Nanoscale vibration characteristics of multi-layered graphene sheets. Mech. Syst. Signal Process. 29, 251–261.
Lin, R.M., 2015. Elastic buckling behaviour of general multi-layered graphene sheets. AIMS Mater. Sci. 2 (2), 61–78.
Liu, M., Yin, X., Ulin-Avila, E., Geng, B., Zentgraf, T., Ju, L., et al., 2011. A graphene-based broadband optical modulator. Nature 474 (7349), 64–67.
Liu, Z., Zhou, H., Lim, Y.S., Song, J.H., Piao, L., Kim, S.H., 2012. Synthesis of silver nanoplates by two-dimensional oriented attachment. Langmuir 28 (25), 9244–9249.
Loomis, J., Panchapakesan, B., 2012. Dimensional dependence of photomechanical response in carbon nanostructure composites: a case for carbon-based mixed-dimensional systems. Nanotechnology 23 (21), 215501.
Loomis, J., King, B., Burkhead, T., Xu, P., Bessler, N., Terentjev, E., Panchapakesan, B., 2012. Graphene-nanoplatelet-based photomechanical actuators. Nanotechnology 23 (4), 045501.
Loomis, J., King, B., Panchapakesan, B., 2012. Layer dependent mechanical responses of graphene composites to near-infrared light. Appl. Phys. Lett. 100 (7), 073108.
Loomis, J., Fan, X., Khosravi, F., Xu, P., Fletcher, M., Cohn, R.W., Panchapakesan, B., 2013. Graphene/elastomer composite-based photo-thermal nanopositioners. Sci. Rep. 3.
Lopez-Urias, F., Rodriguez-Manzo, J., Munoz-Sandoval, E., Terrones, M., Terrones, H., 2006. Magnetic response in finite carbon graphene sheets and nanotubes. Opt. Mater 29, 110.
Lu, S., Panchapakesan, B., 2007. All-optical micromirrors from nanotube MOMS with wavelength selectivity. J. Microelectromech.l Syst. 16 (6), 1515–1523.
Lu, S., Panchapakesan, B., 2007. Photomechanical responses of carbon nanotube/polymer actuators. Nanotechnology 18, 305502.
Lu, P., Zhang, P.Q., Lee, H.P., Wang, C.M., Reddy, J.N., 2007. Non-local elastic plate theories. Proc. R. Soc. A Math. Phys. Eng. Sci. 463 (2088), 3225–3240.
Malekzadeh, P., Shojaee, M., 2013. Free vibration of nanoplates based on a nonlocal two-variable refined plate theory. Compos. Struct. 95, 443–452.
Meyer, J.C., Geim, A.K., Katsnelson, M.I., Novoselov, K.S., Booth, T.J., Roth, S., 2007. The structure of suspended graphene sheets. Nature 446 (7131), 60–63.
Mohammadi, M., Ghayour, M., Farajpour, A., 2013. Free transverse vibration analysis of circular and annular graphene sheets with various boundary conditions using the nonlocal continuum plate model. Compos. Part B Eng. 45 (1), 32–42.
Murmu, T., Adhikari, S., 2010. Nonlocal transverse vibration of double-nanobeam-systems. J. Appl. Phys. 108, 083514.
Murmu, T., Adhikari, S., 2011. Nonlocal vibration of bonded double-nanoplate-systems. Compos. Part B Eng. 42 (7), 1901–1911.
Murmu, T., McCarthy, M.A., Adhikari, S., 2012. Vibration response of double-walled carbon nanotubes subjected to an externally applied longitudinal magnetic field: a nonlocal elasticity approach. J. Sound Vib. 331 (23), 5069–5086.
Murmu, T., McCarthy, M.A., Adhikari, S., 2012. Nonlocal elasticity based magnetic field affected vibration response of double single-walled carbon nanotube systems. J. Appl. Phys. 111 (11), 113511.
Murmu, T., McCarthy, M.A., Adhikari, S., 2013. In-plane magnetic field affected transverse vibration of embedded single-layer graphene sheets using equivalent nonlocal elasticity approach. Compos. Struct. 96, 57–63.
Nair, R.R., Tsai, I.L., Sepioni, M., Lehtinen, O., Keinonen, J., Krasheninnikov, A.V., et al., 2013. Dual origin of defect magnetism in graphene and its reversible switching by molecular doping. Nat. Commun. 4.
Narendar, S., Gupta, S.S., Gopalakrishnan, S., 2012. Wave propagation in single-walled carbon nanotube under longitudinal magnetic field using nonlocal Euler–Bernoulli beam theory. Appl. Math. Model. 36 (9), 4529–4538.

Ni, Z., Bu, H., Zou, M., Yi, H., Bi, K., Chen, Y., 2010. Anisotropic mechanical properties of graphene sheets from molecular dynamics. Phys. B Condens. Matter 405 (5), 1301–1306.
Ning, G., Xu, C., Hao, L., Kazakova, O., Fan, Z., Wang, H., et al., 2013. Ferromagnetism in nanomesh graphene. Carbon 51, 390–396.
Olsen, R., van Gelderen, R., Smith, C.M., 2013. Ferromagnetism in ABC-stacked trilayer graphene. Phys. Rev. B 87 (11), 115414.
Peddieson, J., Buchanan, G.R., McNitt, R.P., 2003. Application of nonlocal continuum models to nanotechnology. Int. J. Eng. Sci. 41, 305–312.
Peng, F., 2011. Magnetic field induced thermal effect of phonons in graphene. Phys. Status Solidi B Basic Solid State Phys. 248, 1388.
Pesin, D., MacDonald, A.H., 2012. Spintronics and pseudospintronics in graphene and topological insulators. Nat. Mater. 11 (5), 409–416.
Pouresmaeeli, S., Ghavanloo, E., Fazelzadeh, S.A., 2013. Vibration analysis of viscoelastic orthotropic nanoplates resting on viscoelastic medium. Compos. Struct. 96, 405–410.
Pradhan, S.C., Kumar, A., 2011. Vibration analysis of orthotropic graphene sheets using nonlocal elasticity theory and differential quadrature method. Compos. Struct. 93 (2), 774–779.
Pradhan, S.C., Phadikar, J.K., 2009. Nonlocal elasticity theory for vibration of nanoplates. J. Sound Vib. 325 (1), 206–223.
Pumera, M., Ambrosi, A., Bonanni, A., Chng, E.L.K., Poh, H.L., 2010. Graphene for electrochemical sensing and biosensing. TrAC Trends Anal. Chem. 29 (9), 954–965.
Qian, D., Dickey, E.C., Andrews, R., Rantell, T., 2000. Load transfer and deformation mechanisms in carbon nanotube-polystyrene composites. Appl. Phys. Lett. 76, 2868–2870.
Ramanathan, T., Abdala, A.A., Stankovich, S., Dikin, D.A., Herrera-Alonso, M., Piner, R.D., et al., 2008. Functionalized graphene sheets for polymer nanocomposites. Nat. Nanotechnol. 3 (6), 327–331.
Reddy, J.N., 2006. Theory and Analysis of Elastic Plates and Shells. CRC Press.
Reddy, J.N., 2007. Nonlocal theories for buckling bending and vibration of beams. Int. J. Eng. Sci. 45, 288–307.
Sandler, J., Shaffer, M.S.P., Prasse, T., Bauhofer, W., Schulte, K., Windle, A.H., 1999. Development of a dispersion process for carbon nanotubes in an epoxy matrix and the resulting electrical properties. Polymer 40, 5967–5971.
Shahil, K.M., Balandin, A.A., 2012. Graphene–multilayer graphene nanocomposites as highly efficient thermal interface materials. Nano Lett. 12 (2), 861–867.
Shen, L., Shen, H.S., Zhang, C.L., 2010. Temperature-dependent elastic properties of single layer graphene sheets. Mater. Des. 31 (9), 4445–4449.
Shen, H.S., Shen, L., Zhang, C.L., 2011. Nonlocal plate model for nonlinear bending of single-layer graphene sheets subjected to transverse loads in thermal environments. Appl. Phys. A 103 (1), 103–112.
Shizuya, K., 2007. Electromagnetic response and effective gauge theory of graphene in a magnetic field. Phys. Rev. B 75.
Singh, S., Patel, B.P., 2016. Nonlinear dynamic response of single layer graphene sheets using multiscale modelling. Eur. J. Mech. A Solids 59, 165–177.
Stankovich, S., Dikin, D.A., Dommett, G.H., Kohlhaas, K.M., Zimney, E.J., Stach, E.A., et al., 2006. Graphene-based composite materials. Nature 442 (7100), 282–286.
Wang, Q., Liew, K.M., 2007. Application of nonlocal continuum mechanics to static analysis of micro- and nano-structures. Phys. Lett. A 363, 236–242.
Wang, Y., Huang, Y., Song, Y., Zhang, X., Ma, Y., Liang, J., et al., 2009. Room-temperature ferromagnetism of graphene. Nano Lett. 9, 220.
Wang, Y.Z., Li, F.M., Kishimoto, K., 2011. Thermal effects on vibration properties of double-layered nanoplates at small scales. Compos. Part B 42, 1311–1317.
Yazyev, O., 2010. Emergence of magnetism in graphene materials and nanostructures. Rep. Prog. Phys. 73.
Zhang, L., Huang, H., 2006. Young's moduli of ZnO nanoplates: ab initio determinations. Appl. Phys. Lett. 89 (18), 183111.